# A New General Riemann Solver for the Shallow Water equations, with friction and topography

**Ashwin Chinnayya**[1]
**Alain-Yves Le Roux**[2]

june 1999

[1]G.R.A.M.M. - Dpt. of Mathematics, University Bordeaux I - 33405 Talence - France. E-mail: chinnayy@math.u-bordeaux.fr

[2]G.R.A.M.M. - Dpt. of Mathematics, University Bordeaux I - 33405 Talence - France. E-mail: AY.leroux@u-bordeaux.fr

## Abstract

We consider numerical approximations of a strickly-hyperbolic system with source terms occuring in hydraulics. The interaction of the bottom slope and the friction slope in the Shallow Water equations is a very dominant term which characterises the *well-balanced states*. We have thought it would be interesting to deal with these so-called *balance laws* with a new numerical processing. At the end, we have been able to run numerical tests. They simulate smooth transitions as well as hydraulic jumps and dry zones.

# Contents

# Introduction

In hydraulics, the source terms correspond to the bottom slope and the friction slope. Their interaction in the Shallow Water equations is a very dominant term which characterizes the well balanced states. In a numerical simulation by a splitting technique for instance, it is difficult to reproduce these equilibra and maintain them for a large number of timesteps, or at least, to avoid a stable equilibrum to be disturbed and destabilized.

A new Riemann solver has been generated and tested. The effects of the source terms of friction and bottom slope are concentrated at the borders of each space cell. At first, a bed slope with friction will be analysed. And all the configurations have then been investigated. This original point of view has enabled us to cope with the phenomenon of stationary shock or hydraulic jump.

A well balanced solver has been built and every situation can be handled.

We have been able to simulate different hydraulic phenomenon such as the hydralic bores and the hydraulic jumps, the presence of dry zone and the generation of dry zone, dynamic waves, and so forth. Several tests show that the solver is endowed with the *Well-Balanced* property which is not shared by most of the numerical methods.

# Chapter 1

# The Shallow Water Equations

In this chapter, the Shallow Water Equations are introduced.

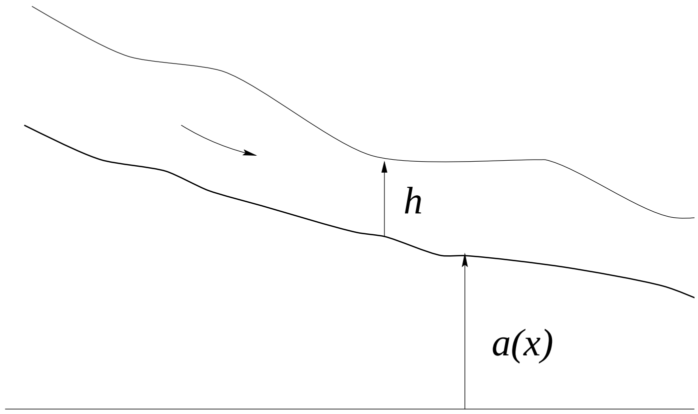


Figure 1.1: Hydraulic flow

## 1.1 Physical Model

We consider a field of vectors $\overrightarrow{V} = \begin{pmatrix} u \\ w \end{pmatrix}$ with

- $u$ being the X-coordinate of the velocity,
- $w$ being the Y-coordinate of the velocity.

The equations can be worked out from the Euler equations for an incompressible fluid. On the first hand, we must consider the incompressibility condition

$$\frac{\partial u}{\partial x} + \frac{\partial w}{\partial z} = 0 \tag{1.1}$$

and on the other hand, the momentum equations

$$\begin{aligned}
\frac{\partial u}{\partial t}+u\frac{\partial u}{\partial x}+w\frac{\partial u}{\partial z} &= -\frac{P_x}{\rho} && (1.2)\\
\frac{\partial w}{\partial t}+u\frac{\partial w}{\partial x}+w\frac{\partial w}{\partial z} &= -\frac{P_z}{\rho}-g && (1.3)
\end{aligned}$$

If we consider that the pressure force is hydrostatic, the dependant variable of the pressure will be the depth of the free-surface flow $h$.

$$\nabla p = -\rho g \nabla (h+a) \text{ such as } \begin{cases} \rho \sim 10^3 \text{ for water ( MKS units ),} \\ g = 9.81 \text{ constant of gravity.} \end{cases} \qquad (1.4)$$

We notice that the equation (1.4) can replace the second dynamic equation. We have assumed that the vertical variations of the speed are negligible compared to the gradient of the pressure.

## 1.2 Boundary Conditions

The bottom is impermeable and we express the fact that we are dealing with a free-surface flow.

$$\begin{cases} w(a+h) = \dfrac{d(a+h)}{dt} = \dfrac{\partial(a+h)}{\partial t} + u(a+h)\dfrac{\partial(a+h)}{\partial x} \\ w(a) = \dfrac{da}{dt} = \dfrac{\partial a}{\partial t} + u(a)\dfrac{\partial a}{\partial x} = u(a)\dfrac{\partial a}{\partial x} \end{cases} \qquad (1.5)$$

## 1.3 The differential form of the Shallow Water equations

We integrate (1.1) and (1.2) with respect to the variable $z$.
Hence (1.1) becomes

$$\int_a^{a+h} (u_x + w_z) dz = 0$$

i.e.

$$\frac{\partial}{\partial x}\Big(\int_a^{a+h} u dz\Big) - \{u(a+h)\frac{\partial(a+h)}{\partial x} - u(a)\frac{\partial a}{\partial x}\} + \{w(a+h) - w(a)\} = 0$$

We denote

$$\tilde{u} = \frac{1}{h}\int_a^{a+h} u dz$$

then with the help of the boundary conditions, we get

$$h_t + (h\tilde{u})_x = 0 \qquad (1.6)$$

If we proceed like previously for the dynamic equation, we obtain

$$\begin{aligned}
(h\tilde{u})_t + (h\tilde{u^2})_x &= -gh\frac{\partial(h+a)}{\partial x} \\
&\quad + u(a+h)\Big(\frac{\partial(h+a)}{\partial t} + u(a+h)\frac{\partial(h+a)}{\partial x} - w(a+h)\Big)
\end{aligned}$$

and with the help of the boundary conditions,

$$(h\tilde{u})_t + (h\tilde{u^2})_x \quad = \quad -gh\frac{\partial(h+a)}{\partial x} \tag{1.7}$$

Thereafter, one makes the following approximation

$$\tilde{u}^2 \approx \tilde{u^2}$$

The Cauchy-Schwartz inequality tells us

$$\tilde{u}^2 = \left|\frac{1}{h}\int_a^{a+h} udz\right|^2 \leq \frac{1}{h}\int_a^{a+h} u^2 dz = \tilde{u^2}$$

Note that this last approximation can be seen as the contribution of a friction phenomenon.

## 1.4 The Friction Slope

Up to now, we have implied that water was a perfect fluid, we have not considered that there might be friction.

Therefore, we must add to the previous equations a friction source term. The friction slope is intended to model boundary friction and turbulence. These are empirical laws which were originally developped for use with steady state flow.

Then after identifying $\tilde{u}$ and $u$, the system becomes

$$\boxed{\begin{array}{c} h_t + (hu)_x = 0 \\ (hu)_t + (hu^2)_x + g\Big(\dfrac{h^2}{2}\Big)_x = -gha_x - \dfrac{g}{C^2}u|u| \end{array}}$$

$C$ is the Chezy coefficient. We assume that our model is very simple and does not include the concept of conveyance. In this report, the following expression will be often used $k = \dfrac{g}{C^2} > 0$.

## 1.5 Steady and Uniform Flow

The flow is steady : $\dfrac{\partial}{\partial t} = 0$ and uniform : $\dfrac{\partial}{\partial x} = 0$.

Given a positive flow rate on a decreasing slope with a constant Chezy coefficient, the system of equations reduces to

$$u = C\sqrt{|a_x|h}$$

which is a kind of Chezy formula. For the convenience of our calculations, we have preferred the following expression

$$\boxed{u = \beta c}$$

such as

$$\begin{cases} \beta = \sqrt{\dfrac{|a_x|}{k}} \\ \\ c = \sqrt{gh} \end{cases} \tag{1.8}$$

Thus, the *normal depth* in our model is defined to be

$$h_o = \left(\frac{1}{\beta}\right)^{\frac{1}{3}} \left(\frac{B^2}{g}\right)^{\frac{1}{3}} \tag{1.9}$$

# Chapter 2

# The Conservative Form

The Shallow Water equations whithout source terms can be written as follows

$$h_t + (hu)_x = 0 \tag{2.1}$$
$$(hu)_t + (hu^2 + g\frac{h^2}{2})_x = 0 \tag{2.2}$$

with piecewise constant initial data of the form

$$(h_o(x), u_o(x)) = \begin{cases} (h_d, u_d) & , x > 0 \\ (h_g, u_g) & , x < 0 \end{cases}$$

## 2.1 Characteristics Fields

If we suppose $h \neq 0$, the initial system can be written in the following non-conservative form

$W_t + A(W)W_x = 0, \quad W = \begin{pmatrix} h \\ u \end{pmatrix}$ i.e.

$$\begin{pmatrix} h_t \\ u_t \end{pmatrix} + \begin{pmatrix} u & h \\ g & u \end{pmatrix} \cdot \begin{pmatrix} h_x \\ u_x \end{pmatrix} = \begin{pmatrix} 0 \\ 0 \end{pmatrix}$$

The eigenvalues of the jacobian $A$ are the roots of the polynom : $(u - \lambda)^2 - gh = 0$ i.e. $\lambda = u \pm c$ , ( $c$ the wave celerity given by $c = \sqrt{gh}$ ) . These two eigenvalues give the characteristic speeds.

These waves are genuinely non linear.

## 2.2 Analysis of the Rarefaction Waves

We consider a regular wave and write $u$ as a function of $h$ : $u(h)$. We get the following system

$$\begin{pmatrix} 1 & u + hu' \\ u + hu' & u^2 + 2uu'h + gh \end{pmatrix} \cdot \begin{pmatrix} h_t \\ h_x \end{pmatrix} = \begin{pmatrix} 0 \\ 0 \end{pmatrix}$$

Hence, if we want the solution to be nonuniform and/or unsteady, we need the matrix to be singular so

$$(hu')^2 = gh \tag{2.3}$$

If $h \neq 0$

$$u' = s\sqrt{\frac{g}{h}},\ s \in \{-1, 1\}$$

Then $u = u_o + 2s(c - c_o)$ across $u + sc$ ( recall $c = \sqrt{gh}$ ).

If $s = -1$, then $h_t + (u - c)h_x = 0$ and $u = u_g - 2(c - c_g)$. After some manipulations, we obtain

$$h_t + f'(h)h_x = 0 \text{ with } f'(h) = u - c = u - hu' = (u_g + 2\sqrt{gh_g} - 3\sqrt{gh})$$

Therefore the flux fonction is strickly concave. As $f''(h).h_x \geq 0$ on a rarefaction wave, we get a *decreasing rarefaction wave*

$$u = u_g + 2(c - c_g),\ \forall 0 < c < c_g$$

If $s = +1$, the same analysis can be repeated for the wave of speed $u + c$ and this time, we get an *increasing rarefaction wave*

$$u = u_d - 2(c - c_d),\ \forall 0 < c < c_d$$

The two Riemann Invariants are : $R_1 = u - 2\sqrt{gh}$ and $R_2 = u + 2\sqrt{gh}$. In addition, we obtain the *characteristic equations*

$$\begin{cases} (R_1)_t + \lambda_1 (R_1)_x = 0 \text{ , pour } \lambda_1 = u - \sqrt{gh} \\ (R_2)_t + \lambda_2 (R_2)_x = 0 \text{ , pour } \lambda_2 = u + \sqrt{gh} \end{cases}$$

If $h = 0$

The speed $u$ will be chosen in order to preserve the monotony of $u$ as a function of $h$ and to respect $hu = 0$.

## 2.3 Analysis of Shocks Waves

We denote by $(h^-, u^-)$ and $(h^+, u^+)$ the states on each side of the shock wave. Here $\overline{u} = \frac{1}{2}(u_+ + u+)$ , $\overline{h} = \frac{1}{2}(h_+ + h+)$ ,
$\triangle q$ the jump of a quantity i.e. $\triangle q = q^+ - q^-$, $\triangle u = u^+ - u^-$, $\triangle h = h^+ - h^-$ and $\dot{x}$ its velocity. Application of the Rankine-Hugoniot conditions yields

$$\dot{x}\triangle u = \triangle hu \quad ; \quad \dot{x}\triangle hu = \triangle\big(hu^2 + g\frac{h^2}{2}\big) \tag{2.4}$$

so the velocity of the shock and the compatibility relation are

$$\dot{x} = \overline{u} + \overline{h}\frac{\triangle u}{\triangle h} \tag{2.5}$$

$$\frac{\triangle hu}{\triangle h} = \frac{\triangle\big(hu^2 + g\frac{h^2}{2}\big)}{\triangle hu} \tag{2.6}$$

Performing some algebraic manipulations one obtains

$$(\triangle hu)^2 = \triangle h \triangle(hu^2) + g\triangle h\triangle(\frac{h^2}{2}) \tag{2.7}$$

i.e.

$$h_+h_-(\triangle u)^2 \quad = \quad g\overline{h}(\triangle h)^2 \tag{2.8}$$

This leads to the following expressions

$$\left\{\begin{array}{lcl} \triangle u & = & s\sqrt{\dfrac{g\overline{h}}{h_+h_-}}\triangle h \ , s \in \{-1,1\} \\ \dot{x} & = & \overline{u} + s\overline{c} \ , \ \overline{c} = \overline{h}\sqrt{\dfrac{g\overline{h}}{h_+h_-}}\triangle h \end{array}\right. \tag{2.9}$$

The two values of $s$ characterize the two waves.

If $\underline{s = -1}$, one gets $\dot{x} = \overline{u} - \overline{c}$. That characterizes the 1-wave. We have an *increasing shock wave* in respect to the spatial variable $x$.

If $\underline{s = +1}$, one gets $\dot{x} = \overline{u} + \overline{c}$. That characterizes the 2-onde. We have a *decreasing shock wave* in respect to the spatial variable $x$.

## 2.4 Synthesis

As a consequence, the relationships between the primitive variables across the two waves are

$$c = \sqrt{gh} \ , \ x^+ = max(x,0) \ , \ x^- = min(x,0)$$

$$\left\{\begin{array}{lcl} (R_g): \ u & = & u_g - 2(c - c_g)^- - \sqrt{\dfrac{c^2 + c_g^2}{2}\dfrac{(c^2 - c_g^2)^+}{cc_g}} \\ (R_d): \ u & = & u_d + 2(c - c_d)^- + \sqrt{\dfrac{c^2 + c_d^2}{2}\dfrac{(c^2 - c_d^2)^+}{cc_d}} \end{array}\right. \tag{2.10}$$

The Riemann problem has given birth to an intermediate state which will be named $S$ and which lies between the two waves.

We can fairly think that hydraulics will generate no strong shocks. Therefore, in a numerical point of view, one can assume *a priori* that both non-linear waves are ruled by the Riemann invariants that is

$$\left\{\begin{array}{lcl} (R_g'): \ u & = & u_g - 2(c - c_g) \\ (R_d'): \ u & = & u_d + 2(c - c_d) \end{array}\right. \tag{2.11}$$

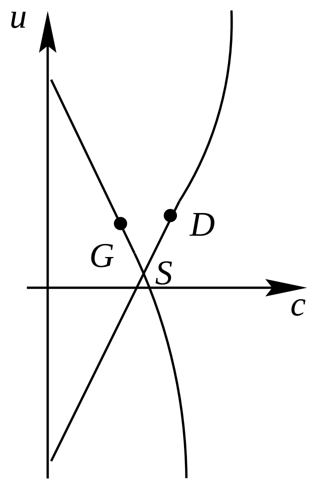


Figure 2.1: Riemann Invariants in the Phase Plane

# Chapter 3

# The Well Balanced Solver for the Shallow Water Equations

We write the Shallow Water equations with source terms.
They can be written,

$$h_t + (hu)_x = 0 \tag{3.1}$$

$$(hu)_t + (hu^2 + g\frac{h^2}{2})_x = -gha_x - ku|u| \tag{3.2}$$

with $a(x)$ the bottom slope, $k = \dfrac{g}{C^2}$ , $C$ the Chezy coefficient, $h = h(x,t)$ the depth, $u = u(x,t)$ the velocity.

On the one hand, most classical schemes make the grid spacing in time become very small as the bottom slope and the friction slope are treated as source terms in a splitting technique for instance. And on the other hand, the equilibrum between these terms and the gradient of pressure is destroyed, therefore it is very difficult for them to cope with nonuniform stationnary solutions.

## 3.1 Analysis of a constant bed slope with slope friction

The Riemann problem consists of the previous system with piecewise constant initial data of the form

$$(h(x,0), u(x,0), a(x), k(x)) = \begin{cases} (h_d, u_d, a_d, k) & \text{for } x > 0 \\ (h_g, u_g, a_g, k) & \text{for } x < 0 \end{cases}$$

Of course, this implies that we must investigate the fact that a product of distributions in $\mathcal{D}'$ $ha_x$ might happen( $h$ can be discontinuous ). This product will be interpretated in the following manner. We will consider the case of the following bottom profile

$$a_\epsilon = \begin{cases} a_g & \text{for } x \le 0 \\ a_g - \dfrac{x}{\epsilon}(a_g - a_d) & \text{for } 0 \le x \le \epsilon \\ a_d & \text{for } x \ge \epsilon \end{cases}$$

With regard to the friction coefficient $k = \dfrac{d}{dx}(kx)$, we follow the ideas of [6]. Then $x \mapsto x$ will be approximated by the piecewise constant function $x \approx \triangle x E(\dfrac{x}{\triangle x}), E(x)$

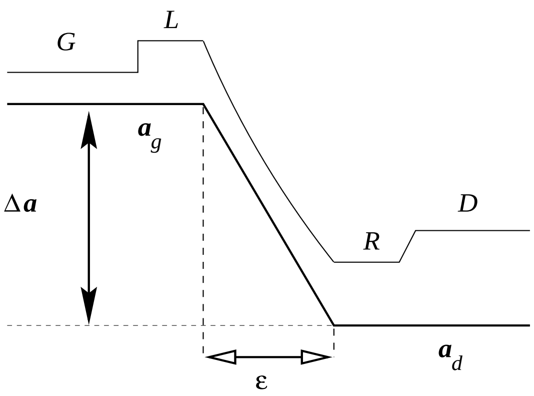


Figure 3.1: Constant Bed Slope

the integer part of $x$,

$$k \approx k\triangle x \frac{d}{dx} E(\frac{x}{\triangle x})$$

i.e.

$$k \approx K'(x) \text{ with } K(x) = k\triangle x E\big(\frac{x}{\triangle x}\big)$$

Of course, this implies that we must investigate the fact that a product of distributions in $\mathcal{D}'$ $u|u|k$ might happen( $u$ can be discontinuous ). This product will be interpretated in the following manner. We will consider the case of the following friction coefficient :

$$K_\epsilon(x) = \begin{cases} nk\triangle x & \text{for } x \leq 0 \\ nk\triangle x + \dfrac{kx}{\epsilon}\triangle x & \text{for } 0 \leq x \leq \epsilon \\ (n+1)k\triangle x & \text{for } x \geq \epsilon \end{cases}$$

such as $n = E\big(\dfrac{x}{\triangle x}\big)$ and

$$k_\epsilon = K'_\epsilon(x)$$

whose jump is $k\triangle x$. For simplicity, we have supposed $k$ constant. In the general case, we get a jump of the friction coefficient equal to $\dfrac{k_g + k_d}{2}\triangle x$.

The solution $(h_\epsilon, u_\epsilon)$ will be constructed for each $\epsilon$ and afterwards, we will study its limit when $\epsilon$ tends towards zero.

In the following chapter, we will see how all these informations can be exploited in order to build our numerical scheme.

### 3.1.1 Analysis of Shocks

Source terms do not modify the study of weak solutions, and a classical study in the vicinity of a discontinuity leads to the same Rankine-Hugoniot Conditions

$$\dot{x}\triangle h = \triangle hu \text{ , } \dot{x}\triangle hu = \triangle\big(hu^2 + g\frac{h^2}{2}\big)$$

i.e.

$$\Big(\triangle(hu)\Big)^2 = \triangle h \triangle(hu^2 + g\frac{h^2}{2})$$

### 3.1.2 Analysis of a Rarefaction

Anyway, the regular waves can not be obtained like in the homogeneous case. From now on, we suppose $\dfrac{-1}{\epsilon}(g\triangle a + k\triangle xu|u|) \neq 0$ and we write $u$ as a function of $h$

$$u = u(h)$$

We obtain

$$\begin{pmatrix} 1 & u + hu' \\ u + hu' & u^2 + 2uu'h + gh \end{pmatrix} \cdot \begin{pmatrix} h_t \\ h_x \end{pmatrix} = \begin{pmatrix} 0 \\ -g\dfrac{\triangle a}{\epsilon} - \dfrac{k\triangle xu|u|}{\epsilon} \end{pmatrix}$$

We get a linear system to be solved. Nevertheless, the matrix can no longer be singular as this would mean that we are dealing with an uniform and steady flow.

Solving this linear system leads to

$$\begin{cases} \psi'(h)h_t = -\dfrac{1}{\epsilon}\dfrac{d}{dh}(hu(h)) \\ \psi'(h)h_x = \dfrac{1}{\epsilon} \end{cases} \tag{3.3}$$

with $\psi'(h) = \dfrac{h(u')^2 - gh}{gh + k\triangle xu|u|}$

Therefore, $\psi(h)$ satisfies

$$\psi(h) = \Upsilon x + C(t),\ \Upsilon = \frac{1}{\epsilon}$$

As $\psi(h)_{xt} = \psi(h)_{tx}$, we get the following second order ordinary differential equation

$$\frac{d^2}{dh^2} hu(h) = 0$$

which integration is instantaneous

$$hu(h) = Ah + B$$

with $A$ et $B$ reals. We can write

$$\psi(h) = \Upsilon(x - At) + C_o \tag{3.4}$$

It is a travelling wave, which velocity is $A$. We also notice that

$$\psi(h)_t + A\psi(h)_x = 0 \tag{3.5}$$

This means that $\psi(h)$ is a wave which velocity is $A = \dfrac{d}{dh}hu(h)$. If the flow rate is constant, i.e. $A = 0$, one observes a stationnary wave.
Let $A \neq 0$ $A > 0$ for instance. Therefore the rate of change of $\psi$ along the characteristic curve $x = At$ is zero, i.e. $\psi$ is constant along the curve $x = At$. But this contradicts $\psi(h)_x = \dfrac{1}{\epsilon}$ hence $A = 0$.

Therefore, we will focus on stationary waves. Hence, we have the following relations across the discontinuity located at $x = 0$, which gives a *stationary contact discontinuity* or *standing wave*.

$$\begin{cases} hu = C^{ste} = B \\ \psi(h)_x = \dfrac{1}{\epsilon} \end{cases} \tag{3.6}$$

We integrate them over the interval $]0, \epsilon[$. We get two meaningful relations

$$\boxed{\begin{array}{rcl} h_l u_l & = & h_r u_r \\ \psi(h_r) - \psi(h_l) & = & 1 \end{array}}$$

such as

$$\begin{cases} \psi'(h) = \dfrac{h^3 - h_c^3}{sk\triangle x h_c^3 + \triangle a h^3} \\ \\ \text{with } h_c = \left(\dfrac{B^2}{g}\right)^{\frac{1}{3}} \text{ and } s = sgn(B) \end{cases}$$

and where subscripts $r$ and $l$ mean right and left traces. Note that the framed relations do not depend on $\epsilon$ and can be seen as the limit as $\epsilon$ goes to zero.

Thereafter, when the difference $\psi(M) - \psi(N)$ will be considered, $M$ and $N$ are considered to belong to the same flow rate.

On the one hand, we will only consider the case where the bottom is decreasing i.e. $\triangle a = -|\triangle a|$. On the other hand, when the bottom is increasing, we only have to change $x$ into $-x$.

### 3.1.3 Remarks

The flow is classified according to the *Froude number*

$$Fr = \frac{|u|}{c} \text{ such as } c = \sqrt{gh} \tag{3.7}$$

$c$ being the sound speed of the hyperbolic system, here called the critical velocity.

For the case $|u| < c$, one characteristic velocity is negative and one is positive. Hence information is transmitted both downstream and upstream. This type of flow is known as *Subcritical Flow* and occurs when gravitationnal forces dominate over inertial forces.

For the case $|u| > c$, both caracteristics are in the same direction as $u$. Hence information is only transmitted downstream. This type of flow is known as *Supercritical Flow* and occurs when inertial forces dominate over gravitationnal forces.

When $|u| = c$, the flow is known as *Critical Flow*. One characteristic is steady and the other is in the same direction of $u$. This type of flow occurs when inertial forces and gravitationnal forces exactly balance.

**When the flow rate is positive**

$$\left\{\begin{array}{ll} h_c & = \left(\dfrac{B^2}{g}\right)^{\frac{1}{3}} \\ h_o & = \left(\dfrac{1}{\beta^2}\right)^{\frac{1}{3}} h_c \end{array}\right. \tag{3.8}$$

such as

$$\beta = \sqrt{\frac{|\triangle a|}{k\triangle x}} \tag{3.9}$$

$h_c$ is the critical depth, i.e. the Froude number values 1.

If the bottom slope and the friction slope are taken as constants, then $h_o$ is the *normal depth*, which is the depth in a steady and uniform flow . We notice that this normal depth is a discrete version of the normal depth which has been defined at the end of the Chapter 1(1.9). Thereafter, one makes no difference between them.

When,

$$h_o > h_c \text{ or } \beta < 1$$

the slope is said to be *Mild*(cf. figure(3.2)).

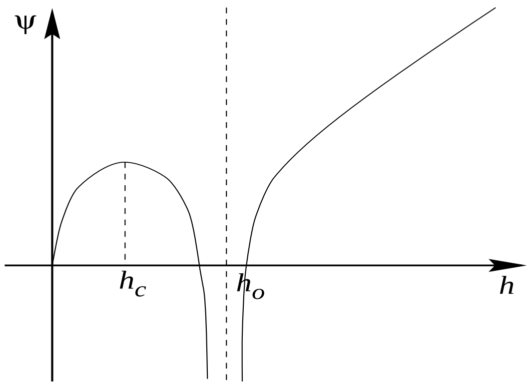


Figure 3.2: $\psi$ ( Mild Slope )

When,

$$h_o < h_c \text{ or } \beta > 1$$

the slope is said to be *Steep*( cf. figure(3.3)).

On the one hand, when

$$u > \beta c \text{ i.e. } h < h_o$$

the slope friction is greater than the bottom slope.

On the other hand, when

$$u < \beta c \text{ i.e. } h > h_o$$

the slope friction is smaller than the bottom slope.

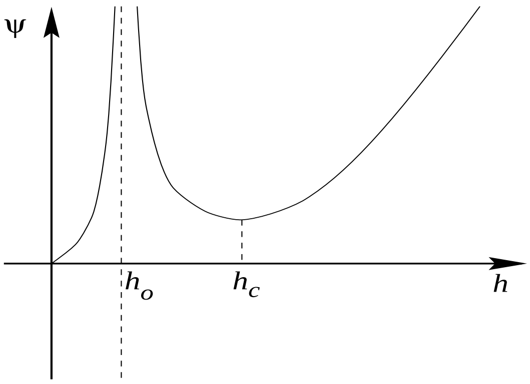


Figure 3.3: $\psi$ ( Steep Slope )

**When the flow rate is negative** $h_c$ has the same expression as before. In this case, $h_o$ is negative and is of no interest(cf. figure3.4).

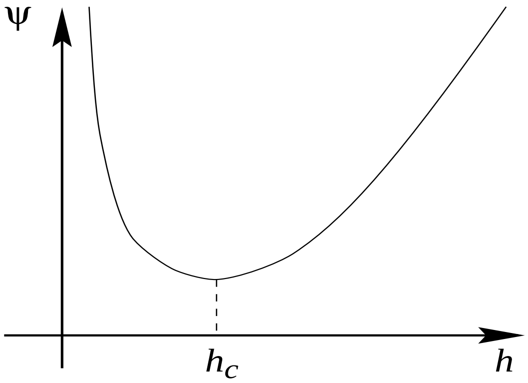


Figure 3.4: $\psi$ ( Adverse Slope )

**Regular Solutions** *Thanks to the equation(3.4), $\psi$ increases as $x$ increases. As $\psi'(h)h_x = \frac{1}{\epsilon} > 0$,*

$$\forall h \in ]inf(h_l, h_r); sup(h_l, h_r)[, \ \psi(h_l) < \psi(h) < \psi(h_r)$$

*i.e.*

*in the interval $]inf(h_l, h_r); sup(h_l, h_r)[$, $\psi'(h)$ must be of constant sign.*

*We see that a regular stationary wave has the two following properties :*

- *the mode( subcritical,mild slope or subcritical,steep slope or supercritical,mild slope or supercritical,steep slope ) can never change on the slope,*
- *a critical velocity can only be reached on the top of the slope.*

## 3.2 The Riemann Problem

The problem can be understood in two ways.

On the one hand, we introduce the augmented problem

$$S_t = 0 \tag{3.10}$$
$$W_t + F(W)_x = S_x \tag{3.11}$$

such as $S$ the source term. Hence the system has three eigenvalues : $u-c, u+c, 0$. The field induced by 0 is obviously linearly degenerate. We have already established two invariants across this standing wave.

On the other hand, the formalism of the well balanced solver leads us to solve the two following initial-boundary problems

1.

$$\begin{cases} h_t + (hu)_x = 0 \\ (hu)_t + (hu^2)_x + g\Big(\dfrac{h^2}{2}\Big)_x = 0 \end{cases} \tag{3.12}$$

with initial and boundary conditions

$$(h,u)(x,0) = (h_g, u_g) \text{ for } x < 0 \tag{3.13}$$
$$(h,u)(0^-,t) = (h_l, u_l) \text{ for } t > 0 \tag{3.14}$$

2.

$$\begin{cases} h_t + (hu)_x = 0 \\ (hu)_t + (hu^2)_x + g\Big(\dfrac{h^2}{2}\Big)_x = 0 \end{cases} \tag{3.15}$$

with initial and boundary conditions

$$(h,u)(x,0) = (h_d, u_d) \text{ for } x > 0 \tag{3.16}$$
$$(h,u)(0^+,t) = (h_r, u_r) \text{ for } t > 0 \tag{3.17}$$

These two initial-boundary problems are linked by two meaningful relations

$$\begin{cases} h_l u_l = h_r u_r \\ \psi(h_r) - \psi(h_l) = 1 \end{cases} \tag{3.18}$$

Therefore each problem can give birth to two waves. Hence our Riemann solver must deal with a priori five waves on the whole -we have included the standing wave in the enumeration.

Let us imagine what will happen if our Riemann problem gives birth to five waves. In this situation, the first and the second initial-boundary problems must produce two waves each. But if the first problem generates two waves, the state $L$ needs to be supercritical with a negative velocity. If the second problem generates two waves, the state $R$ needs to be supercritical with a positive velocity. Therefore, $u_l < 0$ and $u_r > 0$, which is impossible as $h_l u_l = h_r u_r$ implies that the two velocities $u_r, u_l$ are of the same sign. Hence, our Riemann problem can only generate 4 waves at the most. And the formalism of our well balanced solver can generate 3 intermediate states at the most.

The first point of view is not able to consider the solutions on the whole, the nonlinear resonant situations for instance. Nevertheless, it enables us to affirm that there is at least 2 intermediate states when regular solutions are investigated across the standing wave.

Finally, when regular solutions are investigated across the standing wave, our Riemann problem will generate at least 2 and at the most 3 intermediate states.

Nevertheless, if the flow rate is positive and the shock wave $u-c$ is stationary i.e. its velocity is nul, we have to choose between the Rankine-Hugoniot relations and the relations which have been constructed in the previous paragraph. Therefore we will try to understand what is happening thanks to the interpretation of the product of distributions which we have exposed at the beginning of this chapter. A special care will be brought to this phenomenon of "hydraulic jump". Let us notice that in this case only one intermediate state is generated.

In conclusion, when an hydraulic jump happens, only one intermediate state is produced by our Riemman initial-boundary problem and on the other hand when regular solutions across the standing wave are investigated, 2 at least and 3 at the most intermediate states will be generated.

## 3.3 The Scheme Construction

Given $\triangle x$ the grid spacing in space and $\triangle t$ the grid spacing in time. The regular mesh is

$$\begin{cases} x_i = i\triangle x, \; x_j = (i+\frac{1}{2})\triangle x \\ M_i = \left](i-\frac{1}{2})\triangle x, (i+\frac{1}{2})\triangle x\right[ \\ t_n = n\triangle t \end{cases}$$

We define

$$V_{\triangle x} = \left\{ v, v_{/M_i} = C^{ste} \right\}$$

and the following projector onto piecewise-constant functions

$$P_{\triangle x} v(x) = \frac{1}{\triangle x} \int_{M_i} v(\eta) d\eta, \text{ for } x \in M_i$$

On the other hand, the bottom slope and the friction slope are also averaged in the following manner

$$a_{\triangle x} = P_{\triangle x} a \text{ and } K_{\triangle x} = P_{\triangle x} K$$

in order to be able to use the Riemann solver that we have worked out.

When the following CFL( Courant Friedrichs Lewy ) condition is fulfilled, it is possible to write down the time average flux functions across each interface and to write down the scheme.

$$\frac{\triangle t}{\triangle x}(|u| + \sqrt{gh}) < 1$$

We define

$$\begin{cases} h_i^n = h^n_{/M_i} \\ j = i + \frac{1}{2} \\ h_j^+ = h\Big((j\triangle x^+, t)\Big) \text{ pour } t \in ]0, \triangle t[ \\ h_j^- = h\Big((j\triangle x^-, t)\Big) \text{ pour } t \in ]0, \triangle t[ \end{cases}$$

and in the same manner $u_i^n, u_j^+, u_j^-, ...$

Thus we intergrate the continuity equation and the dynamic equation and the scheme reduces to

$$\boxed{\begin{array}{lcl} h_i^{n+1} & = & h_i^n - \dfrac{\triangle t}{\triangle x}\Big(h_j^- u_j^- - h_{j-1}^+ u_{j-1}^+\Big) \\ (hu)_i^{n+1} & = & (hu)_i^n - \dfrac{\triangle t}{\triangle x}\Big(h_j^-(u_j^-)^2 + g\Big(\dfrac{h_j^2}{2}\Big)^- - h_{j-1}^+(u_{j-1}^+)^2 - g\Big(\dfrac{h_{j-1}^2}{2}\Big)^+\Big) \end{array}}$$

The velocity can be evaluated as

$$\begin{cases} u_i^{n+1} = \dfrac{(hu)_i^{n+1}}{h_i^{n+1}}, \text{ if } h_i^{n+1} > 0 \\ u_i^{n+1} = 0 \text{ , else} \end{cases}$$

# Chapter 4

# Riemann Problem Analysis

We consider the problem

$$\begin{aligned} h_t + (hu)_x &= 0 &\quad (4.1)\\ (hu)_t + (hu^2 + g\frac{h^2}{2})_x &= -gh\frac{d}{dx}a - u|u|\frac{d}{dx}K_{\triangle x} &\quad (4.2)\end{aligned}$$

with piecewise constant initial data of the form

$$(h_o(x), u_o(x)) = \begin{cases} (h_d, u_d) & , \ x > 0 \\ (h_g, u_g) & , \ x < 0 \end{cases}$$

The initial states will be denoted $G$ and $R$. The intermediate states $(h_l, u_l)$ and $(h_r, u_r)$ will be denoted $L$ and $R$. The solution $(L, R)$ of the Riemann problem has to be numerically evaluated. We will work out the solution in the phase plane.

The two cases *Mild slope* and *Steep slope* will be presented. In each case, regular solutions will be constructed and when this will be impossible, discontinuous solutions will be proposed.

We use the phase plane, the function $\psi$ and the $(x,t)$ space. We will use mostly the remarks of the paragraph "The Riemann Problem" in the previous chapter.

## 4.1 Mild Slope

Hence one gets

$$\begin{cases} \beta < 1 \\ \text{i.e. } h_n > h_c \text{ for a positive flow rate } B > 0 \end{cases} \quad (4.3)$$

One defines the different zones in the phase plane

$$\begin{cases} T^+ = \{(u,c) \ ; \ u > c\} \\ F_f^+ = \{(u,c) \ ; \ c > u > \beta c\} \\ F_t^+ = \{(u,c) \ ; \ \beta c > u > 0\} \\ F^- = \{(u,c) \ ; \ -c < u < 0\} \\ T^- = \{(u,c) \ ; \ u < -c\} \end{cases} \quad (4.4)$$

Moreover, the flow is controlled by the function $\psi$. Given a positive flow rate, one defines

$$\begin{cases} M_1 = \{h; h < h_c\} \\ M_2 = \{h; h_c < h < h_o\} \\ M_3 = \{h; h > h_o\} \end{cases} \quad (4.5)$$

Given a negative flow rate, one defines

$$\begin{cases} H_1 = \{h; h < h_c\} \\ H_2 = \{h; h_c < h\} \end{cases} \tag{4.6}$$

The phase plane is declined in the following way (cf. figure(4.1)).

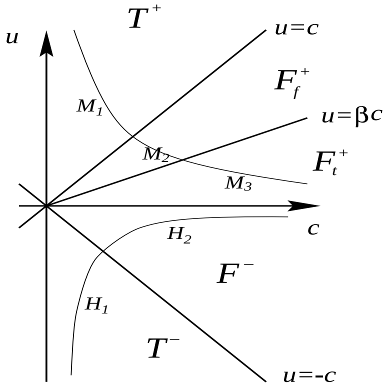


Figure 4.1: Phase Plane

At first, we will try to understand what happens for a positive flow and afterwards the case of an adverse slope will be developped.

### 4.1.1 Regular Solutions for a Positive Flow

On the one hand, regular solutions for a positive flow will be described i.e. $(L, R) \in \{u > 0\}$.

**Supercritical Solutions**

Both waves are upstream(cf. figure(4.2)).

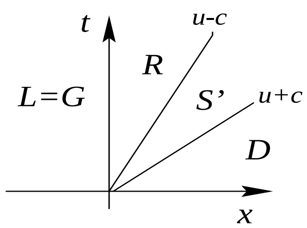


Figure 4.2: Supercritical Solutions

If the point $\boldsymbol{S} \in \boldsymbol{T}^+$ and $\boldsymbol{G} \in \boldsymbol{T}^+$ then we look for a solution in $\boldsymbol{M_1}$(cf. figure(4.3)).

**Case 1'**

$$\begin{cases} L \equiv G \text{ ie } h_l = h_g; u_l = u_g \\ \text{hence } B = h_g u_g \\ R \in M_1 \text{ such as } \psi(h_r) = 1 + \psi(h_g) \end{cases} \tag{4.7}$$

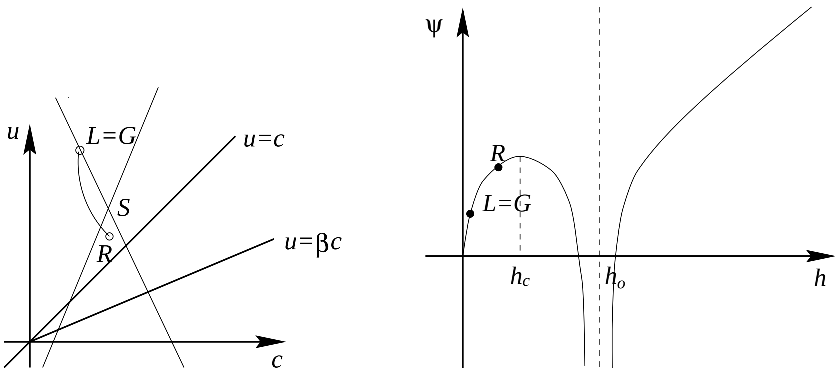


Figure 4.3: Case 1'

We cannot always seek a solution in $M_1$. For this case, a special care will be taken in the next paragraph.

**Subcritical Solutions**

This case happens when information is transmitted both upstream and downstream. Both waves are subcritical(cf. figure(4.4)).

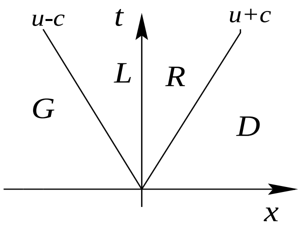


Figure 4.4: Subcritical Solutions

**Cas 1** If the point $\boldsymbol{S} \in \boldsymbol{T}^+$ and ( $\boldsymbol{G} \notin \boldsymbol{T}^+$ or $\boldsymbol{R_d} < \boldsymbol{0}$ ) then we look for a solution in $\boldsymbol{M_2}$.

We consider the following points

$$\begin{cases} N \in R_d \cap \{u = c\} \\ M \in R_g \cap \{uc^2 = u_N c_N^2\} \\ P \in R_g \cap \{u = \beta c\} \end{cases}$$

The Froude numbers of $M$ and $P$ are compared.
If $\underline{Fr(M) < Fr(P)}$ then(cf. figure(4.5))

$$\begin{cases} R \text{ is critical i.e. } R \in \{u = c\} \\ L \in R_g \end{cases}$$

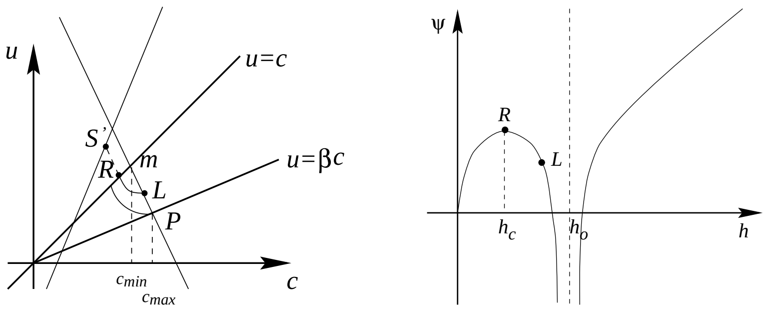


Figure 4.5: Case 1 with R critical

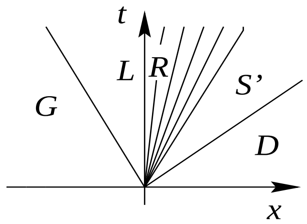


Figure 4.6: Case 1 with R critical in $(x, t)$

Dichotomy will enable us to numerically evaluate the solution. The iterative variable is $c_l = \sqrt{gh_l}$. One considers

$$\begin{cases} m \in R_g \cap \{u = c\} \text{ hence } c_{min} = c_m \\ P \in R_g \cap \{u = \beta c\} \text{ hence } c_{max} = c_P \end{cases}$$

$$\left[\begin{array}{l} c_l = \dfrac{c_{min} + c_{max}}{2}; L \text{ such as } L \in R_g; \\ B = h_l u_l; \\ h_r = \left(\dfrac{B^2}{g}\right)^{\frac{1}{3}}; u_r = \dfrac{B}{h_r} \ (R \in \{u = c\}) \\ \left\{\begin{array}{l} \text{If } \psi(R) - \psi(L) > 1 \text{ then} \\ \quad c_{max} = c \\ \text{Else} \\ \quad c_{min} = c \\ \text{EndIf} \end{array}\right. \end{array}\right. \tag{4.8}$$

One reiterates until convergence. The iterative method is stopped when $|\triangle\psi - 1| < \epsilon$.

One notices that there is always solution. Indeed

$$\left[\begin{array}{l} \text{when the point } L = m \ , \triangle\psi = 0 \\ \text{and when the point L=P } \in \{u = \beta c\}, \triangle\psi = +\infty, \\ \text{then as } \psi \text{ is strickly monotonous on } M_2, \end{array}\right.$$

there is always at least one solution as wished.

If $\underline{Fr(M) > Fr(P)}$ then(cf. figure(4.7))

$$\{\ R \in R_d \cup \{u = c\}; L \in R_g\ \}$$

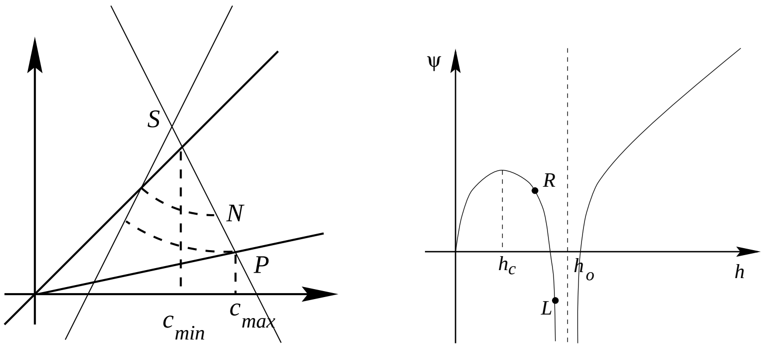


Figure 4.7: Case 1

If we consider the point $M_1 \in R_d \cap \{u = c\}$, we deduce the point $N \in R_g \cap \{uc^2 = u_{M_1} c_{M_1}^2\}$. Then one uses a dichotomy method with the iterative variable being $c_l = \sqrt{gh_l}$.
$m \in R_g \cap \{u = c\}$ then $c_{min} = c_m$ , $P \in R_g \cap \{u = \beta c\}$ then $c_{max} = c_P$

$$\left[\begin{array}{l}
c_l = \dfrac{c_{min} + c_{max}}{2}; L \text{ such as } L \in R_g; \\
B = h_l u_l; \\
\left\{\begin{array}{l}
\text{If } (c_l < c_N) \text{ then} \\
\quad h_r = \left(\dfrac{B^2}{g}\right)^{\frac{1}{3}}; u_r = \dfrac{B}{h_r} \ (R \in \{u = c\}) \\
\text{Else} \\
\quad R \in R_d \cap \{uc^2 = u_l c_l^2\} \\
\text{Endif}
\end{array}\right. \\
\\
\left\{\begin{array}{l}
\text{If } \psi(R) - \psi(L) > 1 \text{ then} \\
\quad c_{max} = c \\
\text{Else} \\
\quad c_{min} = c \\
\text{Endif}
\end{array}\right.
\end{array}\right. \tag{4.9}$$

As for the previous case, one proves that there is at least one solution.

**Case 2 Friction** For this case, both waves are subcritical and we will seek a solution in $\boldsymbol{M_2}$ as the point $\boldsymbol{S} \in \boldsymbol{F_f^+}$. The friction slope is greater than the bottom slope(cf. figure(4.8).

We look for the numerical solution in the same way as in the previous cases. And one easily proves that there is at least one solution.

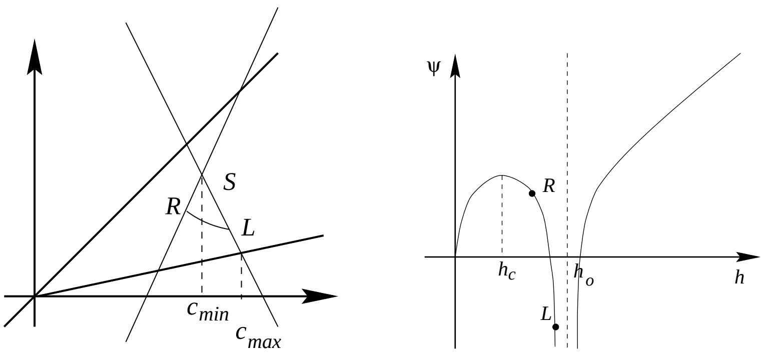


Figure 4.8: Case 2 Friction

**Case 2 Bottom** For this case, both waves are subcritical and we will seek a solution in $\boldsymbol{M_3}$ as the point $\boldsymbol{S} \in \boldsymbol{F_t^+}$. The bottom slope is greater than the friction slope(cf. figure(4.9)

We look for the numerical solution in the same way as in the previous cases. And one easily proves that there is at least one solution.

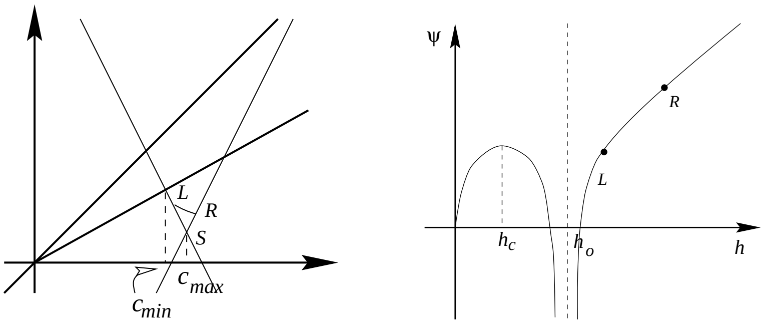


Figure 4.9: Case 2 Bottom

### 4.1.2 Stationary Shock

**Some Hyperbolic**

If $G \in T^+$, one defines

$$D^+ = \{(u,c); hu > h_g u_g\} \tag{4.10}$$
$$D^- = \{(u,c); hu \leq h_g u_g\} \tag{4.11}$$

$L \in D^+$ and $L \neq G$ leads to a nonsense.
Indeed, $\dot{x}(h_l - hg) = (h_l u_l - h_g u_g)$ then $\dot{x} > 0$, hence $L = G$.

Thus, $L$ has to belong to $D^-$. Therefore we will have to look again to all the procedures which have been built in the previous paragraph.

In the previous paragraph, in all cases, one subcritical solution can always be found. But if the source term tends to zero, we have to recover a Riemann solver adapted to the homogeneous problem. Hence if $G$ is supercritical with a positive velocity, one defines the set of points $L$ of the phase plane such as $(u - c)_{GL} > 0$ in order to upwind the information. By doing this, we will see that stationary shocks have to be built on the slope.

**Case 1, Supercritical $\leftrightarrow$ Subcritical**

In the case $\underline{\boldsymbol{G \in T^+} \text{ and } \boldsymbol{S \in T^+}}$, one defines

$$\begin{cases} B_g \text{ the flow rate of } G \\ G^* = B_g \cap R_g \cap F^+ \\ R^* = B_g \cap R_d \\ N \text{ such as } N = \begin{cases} B_g \cap \text{ the } u-c \text{ invariant which contains the point } R^* \text{ if } R^* \in F^+ \\ R^* \text{ else} \end{cases} \\ R' = B_g \cap \{u = c\} \end{cases} \tag{4.12}$$

At first, we will study the case when $\underline{G^* \in F_t^+, R^* \in F_f^+}$.

One has $L = G \in T^+$. At first, a supercritical solution will be seeked(cf. figure(4.2)). There is an intermediate state $S'$ which lies between $R$ and $D$. Indeed $R$ will give birth to a $u-c$ wave which velocity must be positive. Hence the depth of $R$ cannot be greater than the depth of $N$.

When the relations across the standing wave cannot be satisfied this means that there is too much friction. Hence, we seek a subcritical solution.

If $R \in F_f^+$ such as $h_r \in M_3$ then $L \in R_g \cap F_f^+$. Hence $L \in D^+$ which is impossible. And if $(L, R) \in F_t^+$ then we obtain the following inequality $h_r < h_l$ which is impossible as $h_r > h_l$ in $M_3$.

Hence regular solutions are not admissible. Thus we look for stationary discontinuous solutions. If the flow is positive -which is our main hypothesis- the only admissible stationary wave is the wave $u - c$(cf. figure(4.10).

If $R$ does not belong to $R_d$, $R$ will generate a $u - c$ wave which velocity is negative. And that is not acceptable. Hence $R$ belongs to $R_d$.

Therefore when $\epsilon$ tends to zero

$$R = R^* \ ; \ L = G$$

The numerical flux can be known whithout knowning the exact position of the stationary shock into $]0, \epsilon[$ and whithout knowning the two points $A$ and $A'$. Nevertheless we want the relations across the standing wave to be valid. Hence one interpretates

$$\psi(h_r) - \psi(h_l) = (\psi(h_r) - \psi(h_{A'})) + (\psi(h_A) - \psi(h_l))$$

If $K = B_g \cap \{u = \beta c\}$ and $A'$ is $K$, we have $\psi(h_{R^*}) - \psi(h_{A'}) = +\infty$ and $\psi(h_A) - \psi(h_g) \in \mathbb{R}$. When $R$ is $N$, it is the limit of the set of supercritical solutions.

Then the relations across the standing wave are always true.

Finally, in the situation which has been considered, the slope friction prevents the $u-c$ wave -which velocity is nonnegative- to go down the slope. Indeed when the slope friction is too important this wave is trapped in the phenomenon of a stationary shock.

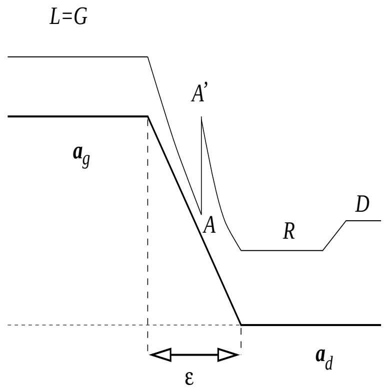


Figure 4.10: Stationary Shock

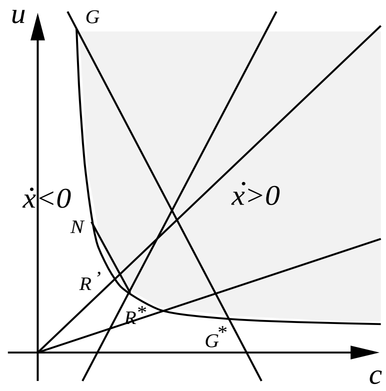


Figure 4.11: $G^* \in F_t^+$, $R^* \in F_f^+$

Hence the numerical algorithm can be written down as follows

$$B = h_g u_g$$
$$\left\{ \begin{array}{l} \text{If } \psi(N) - \psi(G) > 1 \text{ then} \\ \quad \text{Case 1'} \\ \text{Else} \\ \quad \text{Stationary Shock } : L = G; R = R^* \\ \text{Endif} \end{array} \right.$$

The same result can be obtained when $\underline{G^* \in F_t^+, R^* \in F_t^+}$.

When $\underline{G^* \in F_t^+, R^* \in T^+}$ the previous algorithm must be slightly modified. $R'$ plays the same role as $N$.

$$B = h_g u_g$$
$$\begin{cases} \text{If } \psi(R') - \psi(G) > 1 \text{ then} \\ \quad \text{Case 1'} \\ \text{Else} \\ \quad \text{Stationary Shock } : L = G; R = R' \\ \text{Endif} \end{cases}$$

We investigate the case when $\underline{G^* \in F_f^+, R^* \in F_f^+}$.

The regular solutions are the Case 1' and the Case 1. Hence, when no supercritical solution can be found, we look for a subcritical solution. But it seems that no discontinuous solution has to be seeked. Nevertheless when numerical tests are proceeded for some values of $\triangle a$ and $k\triangle x$, we notice that there always exists a $\delta > 0$ such as $\psi(N) - \psi(G) \leq 1 - \delta < 1 < 1 + \delta \leq \psi(R^*) - \psi(G^*)$. In this numerical range, a stationary shock seems to be the right solution.

Indeed during a supercritical flow, the velocity of the wave $u - c$ is positive and during a subcritical flow, the velocity of the wave $u - c$ is negative. Hence when the friction slope is gradually increased, the flow being initially supercritical goes to the stationary phenomenon before going to the subcritical mode.

Therefore the numerical algorithm can be written down as follows

$$B = h_g u_g$$
$$\begin{cases} \text{If } \psi(N) - \psi(G) > 1 \text{ then} \\ \quad \text{Case 1'} \\ \text{Else if } \psi(R^*) - \psi(G^*) > 1 \text{ then} \\ \quad \text{Stationary Shock } : L = G; R = R^* \\ \text{Else} \\ \quad \text{Case 1} \\ \text{Endif} \end{cases}$$

When $\underline{G^* \in F_f^+, R^* \in T^+}$, the previous alogorithm becomes( R' plays the same role as N)

$$B = h_g u_g$$
$$\begin{cases} \text{If } \psi(R') - \psi(G) > 1 \text{ then} \\ \quad \text{Case 1'} \\ \text{Else if } \psi(R') - \psi(G^*) > 1 \text{ then} \\ \quad \text{Stationary Shock} : L = G; R = R' \\ \text{Else} \\ \quad \text{Case 1} \\ \text{Endif} \end{cases}$$

**Case 2 Friction, Supercritical $\leftrightarrow$ Subcritical**

Here, $\underline{\boldsymbol{G \in T^+, S \in F_f^+}}$. For the same reasons as in the previous paragraph, stationary shocks have to be investigated. The notations are those of (4.12). In this case, the solver is built according to the relative position of $G^*$ compared to $S$ in the phase

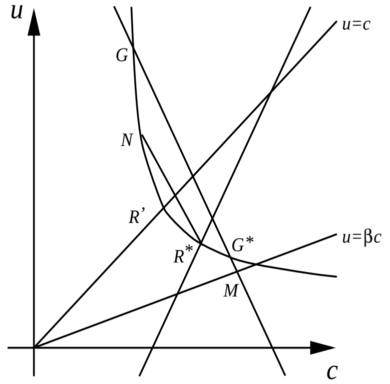


Figure 4.12: Case 2 Friction, Supercritical $\leftrightarrow$ Subcritical

plane. One defines $M = \{u = \beta c\} \cap R_g$.

The algorithm can be written down as follows

$$
\begin{cases}
\text{If } (h_{G^*} < h_S) \text{ then} \\
\quad \text{Case 2 Friction} \\
\\
\text{ElseIf } (h_{G^*} > h_M) \text{ then} \\
\begin{cases}
\text{If } \psi(N) - \psi(G) > 1 \text{ then} \\
\quad \text{Case 1'} \\
\text{Else} \\
\quad \text{Stationary Shock } : L = G; R = R^* \\
\text{Endif}
\end{cases} \\
\\
\text{Else} \\
\begin{cases}
\text{If } \psi(N) - \psi(G) > 1 \text{ then} \\
\quad \text{Case 1'} \\
\text{Elseif } \psi(R^*) - \psi(G^*) < 1 \text{ then} \\
\quad \text{Case 2 friction} \\
\text{Else} \\
\quad \text{Stationary Shock} : L = G; R = R^* \\
\text{Endif}
\end{cases} \\
\text{Endif}
\end{cases}
\tag{4.13}
$$

The figure(4.12) deals with the case when $h_S < h_{G^*} < h_M$.
In this case(4.12), solutions are seeked as follows :

If the slope friction is not very important, we can look for a supercritical solution and the wave $u - c$ is at the right of the discontinuity.

If the slope friction is increased, then a stationary shock happens and the discontinuity wants to trap the wave $u - c$ in the phenomenon of stationary shock.

If the slope friction is very important, the solution will be subcritical and the wave $u - c$ will be at the left of the discontinuity.

### Case 2 Bottom, Supercritical $\leftrightarrow$ Subcritical

Here $\boldsymbol{G} \in \boldsymbol{T}^{+}, \boldsymbol{S} \in \boldsymbol{F}_t^{+}$. The solver can be built by using the same ideas used until now. One defines $M = \{u = \beta c\} \cap R_g$.

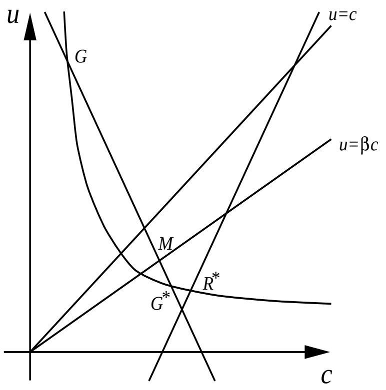


Figure 4.13: Case 2 Bottom, Supercritical $\leftrightarrow$ Subcritical

The algorithm can be written down as follows

$$\left\{\begin{array}{l} \text{If } (h_{G^*} < h_M) \text{ then} \\ \quad \text{Case 2 Bottom} \\ \\ \text{Elseif } (h_S > h_{G^*} > h_M) \text{ then} \\ \left\{\begin{array}{l} \text{If } \psi(R^*) - \psi(G^*) > 1 \text{ then} \\ \quad \text{Case 2 Bottom} \\ \text{Else} \\ \quad \text{Stationary Shock } : L = G; R = R^* \\ \text{Endif} \end{array}\right. \\ \\ \text{Else} \\ \quad \text{Stationary Shock } : L = G; R = R^* \\ \text{Endif} \end{array}\right. \tag{4.14}$$

The figure(4.13) deals with the case where $h_S > h_{G^*} > h_M$.

In this case(4.13), solutions are seeked as follows :

If the bottom slope is not very important, we look for a subcritical solution, therefore the wave $u - c$ is at the left of the discontinuity.

If the bottom slope is increased, we would like to look for a supercritical flow. But friction will catch the wave $u - c$ and this wave will get trapped in the phenomenon of a stationary shock.

### 4.1.3 The Riemann Solver for a Positive Flow

Finally when the flow is positive and $\beta < 1$, the solver can be written down as follows

$$\begin{cases} \text{If } S \in T^+ \text{ then} \\ \begin{cases} \text{If } G \in T^+ \\ \quad \text{Case 1, Supercritical } \leftrightarrow \text{ Subcritical Else} \\ \quad \text{Case 1} \\ \text{Endif} \end{cases} \\ \text{Elseif } S \in F_f^+ \text{ then} \\ \begin{cases} \text{If } G \in T^+ \\ \quad \text{Case 2 Friction, Supercritical} \leftrightarrow \text{Subcritical} \\ \text{Else} \\ \quad \text{Case 2 Friction} \\ \text{Endif} \end{cases} \\ \text{Else} \\ \begin{cases} \text{If } G \in T^+ \\ \quad \text{Case 2 Bottom, Supercritical} \leftrightarrow \text{Subcritical} \\ \text{Else} \\ \quad \text{Case 2 Bottom} \\ \text{Endif} \end{cases} \\ \text{Endif} \end{cases} \tag{4.15}$$

### 4.1.4 Negative Flow

At first, let us consider the case when $R_g = 2\sqrt{gh_g} + u_g > 0$.

If $S \in T^-, D \in T^-$, then the algorithm can be written as follows(cf. figure 4.14)

$$\begin{cases} \text{If } (\psi(h_d) - \psi(h_{L'}) > 1; \text{ such as } B = B_d) \text{ then} \\ \quad \text{Case 3':} \begin{cases} R = D; B = B_d; \\ L \in S_1 / h_d < h_l < h_c = h_{L'} \end{cases} \\ \text{Elseif } (\psi(M) - \psi(N) > 1; \text{ such as } B_M = B_N \text{ ) then} \\ \quad \text{Case 3:} \begin{cases} L \in \{u = -c\} / h_{L'} < h_l < h_M \\ R \in R_d \end{cases} \\ \text{Elseif } (\psi(P) - \psi(K) > 1; \text{ such as } B_M = B_N \text{ ) then} \\ \quad \text{We look for a solution whith a positive flow rate.} \\ \quad \text{The solutions are exactly the same as those of the previous chapter} \\ \text{Endif} \end{cases} \tag{4.16}$$

We always use dichotomy in order to numerically evaluate the solution.
If $S \in F^-$ then we look for a solution such as (cf. figure 4.16)

$$L \in R_d; R \in R_g$$

Here dichotomy is also used.

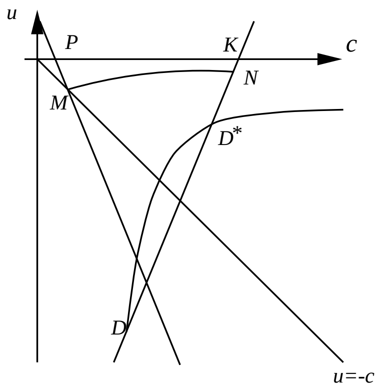


Figure 4.14:

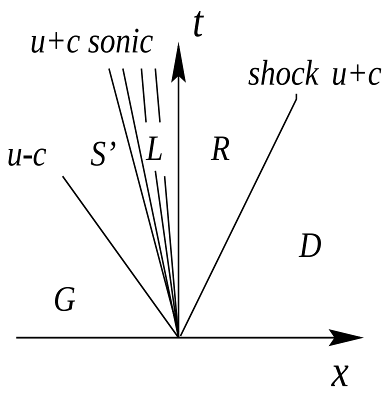


Figure 4.15: Case 3 in (x,t)

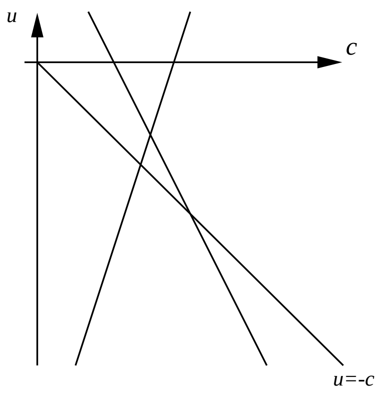


Figure 4.16:

If $R_g < 0$ then one finds itself in the following situation(cf. figure 4.17).

$$\left\{\begin{array}{l} \text{If } D \in T^{+} \text{ and } \psi(D) - \psi(L') > 1( \text{ such as } B_d = B_{L'}) \\ \quad \text{Case 3'} \\ \text{Elseif } (|h_M - h_N| < |\triangle a| \text{ then} \\ \quad \text{Case 3} \\ \text{Else} \\ \quad \text{Reflexion} \left\{\ R = N; L = M\ \right\} \\ \text{Endif} \end{array}\right. \tag{4.17}$$

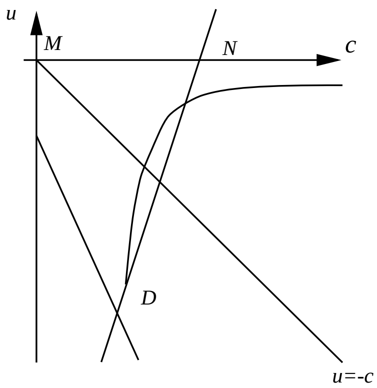


Figure 4.17:

## 4.2 Steep Slope

Hence one gets

$$\begin{cases} \beta > 1 \\ \text{i.e. } h_o < h_c \text{ for a positive flow } B > 0 \end{cases} \tag{4.18}$$

One defines the different zones in the phase plane

$$\begin{cases} T_f^+ = \{(u,c)\ ;\ u > \beta c\} \\ T_t^+ = \{(u,c)\ ;\ c < u < \beta c\} \\ F^+ = \{(u,c)\ ;\ c > u > 0\} \\ F^- = \{(u,c)\ ;\ -c < u < 0\} \\ T^- = \{(u,c)\ ;\ u < -c\} \end{cases} \tag{4.19}$$

Moreover the flow is controlled by the function $\psi$. Given a positive flow rate, one defines

$$\begin{cases} S_1 = \{h; h < h_o\} \\ S_2 = \{h; h_o < h < h_c\} \\ S_3 = \{h; h > h_c\} \end{cases} \tag{4.20}$$

Given a negative flow rate, one defines

$$\begin{cases} H_1 = \{h; h < h_c\} \\ H_2 = \{h; h_c < h\} \end{cases} \tag{4.21}$$

The phase plane is declined in the following way(cf. figure(4.18)).

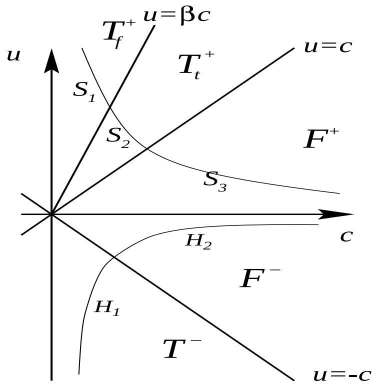


Figure 4.18: Phase Plane

At first, the solutions for a positive flow will be cleared up then the case of an adverse slope will be developped.

### 4.2.1 Regular Solutions for a Positive Flow

**Supercritical Solutions**

Both waves are upstream(cf. figure(4.2))

We will name this case **Case 1'**. If the point $\boldsymbol{S} \in \boldsymbol{T}^+ = \boldsymbol{T}_f^+ \cup \boldsymbol{T}_t^+$ then we have a supercritical solution.

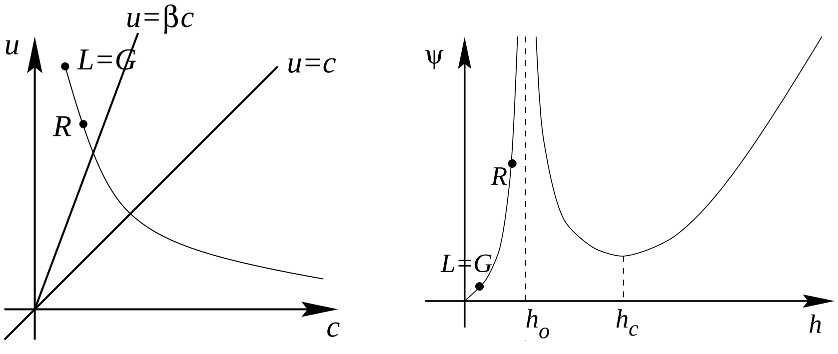


Figure 4.19: Case 1'

If the point $\underline{G \in T_f^+}$, then a solution in $S_1$ can be seeked(cf. figure(4.19))

$$\left\{ \begin{array}{l} L \equiv G \in S_1 \text{ thus } h_l = h_g; u_l = u_g \\ \text{ hence } B = h_g u_g \\ R \in S_1 \text{ such as } \psi(h_r) = 1 + \psi(h_g) \end{array} \right. \tag{4.22}$$

If the point $\underline{G \in T_t^+}$, then we look for a solution in $S_2$(cf. figure(4.20)).

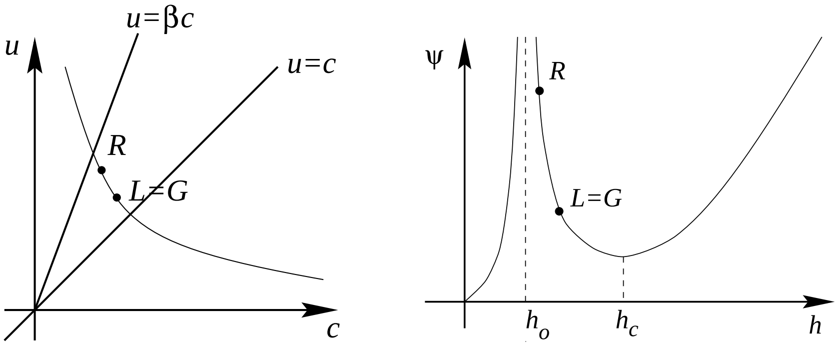


Figure 4.20: Case 1'

$$\left\{ \begin{array}{l} L \equiv G \in S_2 \text{ thus } h_l = h_g; u_l = u_g \\ \text{ hence } B = h_g u_g \\ R \in S_2 \text{ such as } \psi(h_r) = 1 + \psi(h_g) \end{array} \right. \tag{4.23}$$

And if the point $\underline{G \notin T^+}$, we look for a solution(cf. figures(4.21) and (4.22)) such as

$$\left\{ \begin{array}{l} L \in R_g \cap \{u = c\} \text{ hence } L \in S_2 \\ R \in S_2 \cap \{uc^2 = u_l c_l^2\} \end{array} \right. \tag{4.24}$$

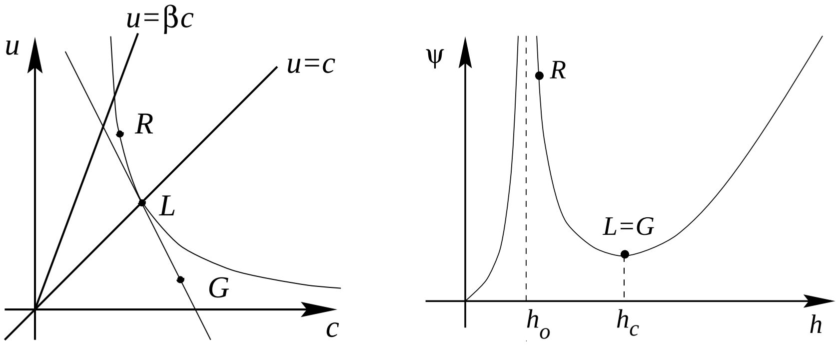


Figure 4.21: Case 1

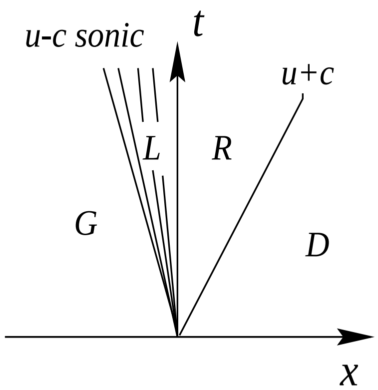


Figure 4.22: Case 1 in (x,t)

**Subcritical Solutions**

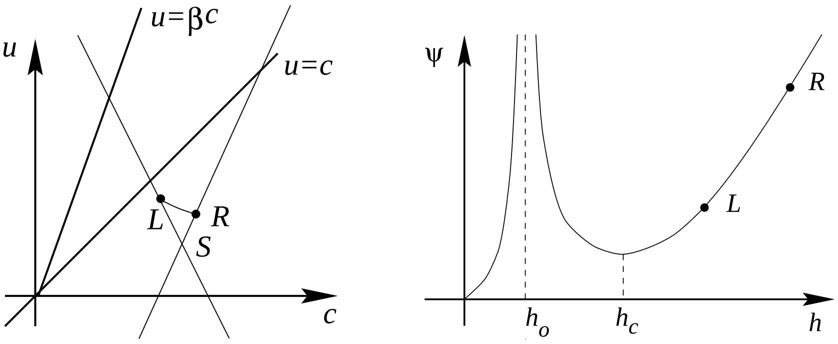


Figure 4.23: Case 2

We name this case **Case 2**( figure(4.23)). If $\boldsymbol{S} \in \boldsymbol{F}^+$ then we look for a solution like described in the figure(4.21) such as $h_l < h_r$. Indeed given a positive flow rate, $(L, R) \in S_3$. We cannot always seek a solution in $S_3$. We will re-examine this problem in the following paragraph.

$m \in \{u = c\} \cap R_g$ hence $c_{min} = c_m$ ; $c_{max} = c_S$
and the algorithm of resolution is based on a dichotomy.

$$\left[\begin{array}{l} c_l = \dfrac{c_{min} + c_{max}}{2}; L \text{ such as } \in R_g; \\ B = B_l \\ R \in R_d \cap B_l; \\ \left\{\begin{array}{l} \text{If } \psi(h_r) - \psi(h_l) > 1 \text{ then} \\ \quad c_{min} = c \\ \text{Else} \\ \quad c_{max} = c \\ \text{Endif} \end{array}\right. \end{array}\right. \tag{4.25}$$

One reiterates until convergence. The iterative procedure is stopped when $\mid \Delta\psi - 1 \mid$ small enough.

### 4.2.2 Stationary Shock

In the case of a mild slope, the phenomenon of a stationary shock seemed to be the most probable solution in some cases. In the case of a steep slope, we investigate when this discontinuous phenomenon can occur.
Therefore, we look again to all the procedures which have been built up to now. We only have to look to the case when the point $G \in T^+$.

**Case 1', Supercritical ↔ Subcritical**

Given $\boldsymbol{S} \in \boldsymbol{T}^+, \boldsymbol{G} \in \boldsymbol{T}_t^+$ the wave $u - c$ generated by the point $R$ cannot have a negative velocity(cf. figure(4.24))

If $\boldsymbol{S} \in \boldsymbol{T}^+, \boldsymbol{G} \in \boldsymbol{T}_f^+$,

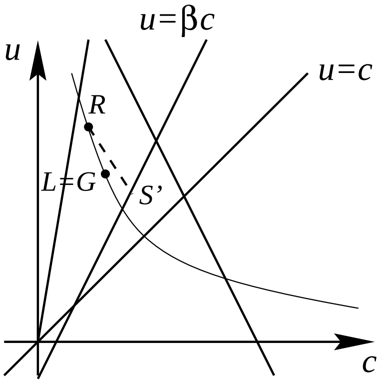


Figure 4.24: Case 1', $S \in T^+$, $G \in T_t^+$

1. If <u>$R^* \in T^+$</u>, we must seek regular solutions $\rightarrow$ Case 1'.

2. If <u>$R^* \in F^+$</u>(figure(4.25)), in order to get $(u-c)_{RS'} > 0$, the depth of $S'$ cannot be greater than the depth of $R^*$ hence the depth of $R \in B_g$ cannot be greater the depth of $N$. Let us notice that if $N \in T_t^+$, $R$ would never reach $N$.

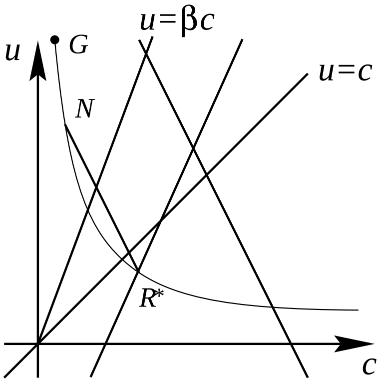


Figure 4.25: Case 1', $G \in T_f^+$, $R^* \in F^+$

The solver can be written down as follows

$$\left\{\begin{array}{l}
\text{If } R^* \in T^+ \\
\quad \text{Case 1'} \\
\text{Else} \\
\left\{\begin{array}{l}
\text{If } N \in T_t^+ \\
\quad \text{Case 1'} \\
\text{Elseif } \psi(h_N) - \psi(h_g) > 1.(\text{ with } B = B_g) \\
\quad \text{Case 1'} \\
\text{Else} \\
\quad \text{Stationary Shock : } L = G; R = R^* \\
\text{Endif}
\end{array}\right. \\
\text{Endif}
\end{array}\right. \tag{4.26}$$

**Case S $\in F^+$ , Supercritical $\leftrightarrow$ Subcritical**

No difficulty is present here. The principles used previously need to be used again.

Let us investigate the case where $G \notin T^+$.

$$\left\{\begin{array}{l} \text{If } \psi(R') - \psi(G') > 1 \text{ then} \\ \quad \text{Case 2} \\ \text{Elseif } (\psi(N) - \psi(G') < 1) \text{ and } N \in T_t^+ \text{ then} \\ \quad \text{Case 1} \\ \text{Else} \\ \quad \text{Stationary Shock: } L = G'; R = R' \\ \text{Endif} \end{array}\right. \tag{4.27}$$

Then if $G \in T_t^+$

$$\left\{\begin{array}{l} \text{If } h_{G^*} < h_S \\ \left\{\begin{array}{l} \text{If } \psi(R^*) - \psi(G^*) > 1 \text{ then} \\ \quad \text{Case 2} \\ \text{Elseif } (\psi(N) - \psi(G) < 1) \text{ and } N \in T_t^+ \text{ then} \\ \quad \text{Case 1'} \\ \text{Else} \\ \quad \text{Stationary Shock: } L = G; R = R^* \\ \text{Endif} \end{array}\right. \\ \text{Else} \\ \quad \text{Stationary Shock: } L = G; R = R^* \\ \text{Endif} \end{array}\right. \tag{4.28}$$

And finally if $G \in T_f^+$

$$\left\{\begin{array}{l} \text{If } h_{G^*} > h_S \text{ then} \\ \quad \text{Stationary Shock: } L = G; R = R^* \\ \text{Elseif } (\psi(R^*) - \psi(G^*) > 1) \text{ then} \\ \quad \text{Case 2} \\ \text{Else} \\ \quad \text{Stationary Shock: } L = G; R = R^* \\ \text{Endif} \end{array}\right. \tag{4.29}$$

We present how the solver look for the solution. On the one hand, we investigate whether a subcritical solution is possible. But if the bottom slope is too important, we must look for a supercritical solution if and only if the wave $(u-c)_{RS}$( figure(4.2) ) remains positive. If the latter proposition is not possible, the phenomenon of a stationary shock will appear.

### 4.2.3 The Riemann Solver for a Positive Flow

Finally when the flow is positive and $\beta > 1$, the solver can be written down as follows

$$
\begin{cases}
\text{If } S \in T^{+} \text{ then} \\
\quad \begin{cases}
\text{If } G \in T^{+} \text{ then} \\
\quad \text{Case 1', Supercritical} \leftrightarrow \text{Subcritical} \\
\text{Else} \\
\quad \text{Case 1} \\
\text{Endif}
\end{cases} \\
\text{Else} \\
\quad \text{Case S} \in F^{+} \text{ , Supercritical} \leftrightarrow \text{Subcritical} \\
\text{Endif}
\end{cases}
\tag{4.30}
$$

### 4.2.4 Negative Flow

For this case, the solver is the same as in the case of the mild slope.

## 4.3 The Riemann Problem in the presence of Dry Zone

Any mathetical model based on the continuum assumption is no longer valid. The structure of the Riemann problem is different from that of the conventional case. The temptation of using small values of depth to simulate dry zone will prove frustating.

The construction of the solver will not be detailed as done previously. The ideas are the same.

#### The Riemann Problem in the presence of Dry Zone

Here, there are two cases. Either the right state is dry or the left state is dry. In either of the two cases, one of the invariants does not exist and therefore the point $S$ does not exist any more.

Suppose the right state to be dry.
One defines $RG = 2\sqrt{gh_g} + u_g$. One knowns that in the homogenous case that if $RG \leq 0$ the numerical flux is nul because water moves away from discontinuity. There is no change for our well balanced scheme.
When $RG > 0$, the solution for the Riemann Solver is generated according to the position of $G$ in the phase plan.

If the left state is dry then one proceeds in the same way. One only needs to reverse the roles.

#### Generation of a Dry Zone

The cavitation is generated if the $S$ point has a negative depth. Therefore the $S$ point does not exist.
Ones defines $RG = 2\sqrt{gh_g} + u_g$ and $RD = 2\sqrt{gh_d} + u_d$.
Three cases must be investigated according to the position of $RG$ and of $RD$ compared to the point $(0, 0)$.

- $RG > 0$

- $RG < 0$ and $RD < 0$
- $RG < 0$ and $RD > 0$

## 4.4 A note on the Numerical Methods used

Using $\psi$ is a costly demanding task in the numerical method. Therefore when we have to evaluate $\triangle\psi$, we use the integration numerical method of Simpson.

Dichotomy is always used in order to evaluate the numerical flux. Indeed, no Newton like method has been proved successful up to now. We have not been able to make them converge. In fact, there are two problems. The first one is when one of the two states is too near of the sonic state and the second one is when one of the depth is near the normal depth. These two states are two singularities of the $\psi$ function.

# Chapter 5

# Numerical Tests

In this chapter, we performed several numerical runs in order to evaluate the performance of the well balanced solver.

On the one hand, we present the steady states in order to show that the scheme will not destroy any equilibra. On the other hand, we look at what happens in the neighbourhood of great variations of topography.

For all the tests, the scheme is run with 75 grid points. The ratio $\triangle t/\triangle x = 0.9$ is kept constant all along the numerical tests. A flow rate is imposed upstream and a free boundary condition downstream.

## 5.1 Uniform and Steady Flow

Given a decreasing bottom slope, a friction slope and a flow rate, the Froude number of the flow can be evaluated as

$$Fr = \beta = \frac{a_x}{k} \simeq \frac{|\triangle a|}{k\triangle x}$$

In the following numerical tests, $k = 0.2$. In order to see whether or not our solver can cope with different hydraulic phenomenons, varying the bottom slope is only needed.

## 5.2 Test 1

The gradient of the channel steadily decreases along the lenght of the reach. The bed slope values 0.05( hence $\beta_{amont} \simeq 0.5$ ) upstream and 0.1 downstream( hence $\beta_{aval} \simeq \sqrt{\frac{1}{2}} \simeq 0.707$ ). Everywhere, the slope is mild.

The flow rate upstream is $12.48ms^{-1}$. The results are shown after 581 iterations of time steps i.e. $t = 350s$. The steady states upstream and downstream are the ones wished. The transition between the two regimes is via a smooth transition.

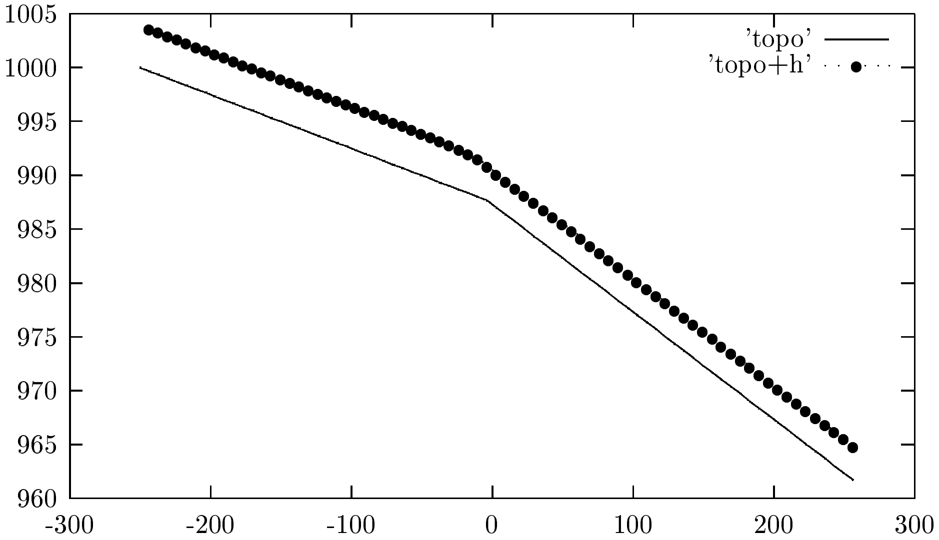
'topo'
'topo+h'
1005
1000
995
990
985
980
975
970
965
960
-300
-200
-100
0
100
200
300

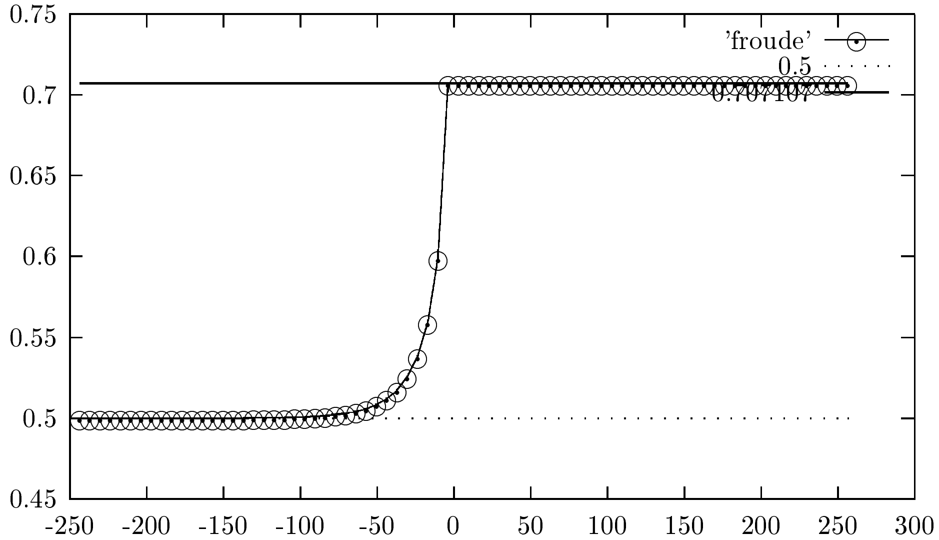
'froude'
0.5
0.707107
0.75
0.7
0.65
0.6
0.55
0.5
0.45
-250
-200
-150
-100
-50
0
50
100
150
200
250
300

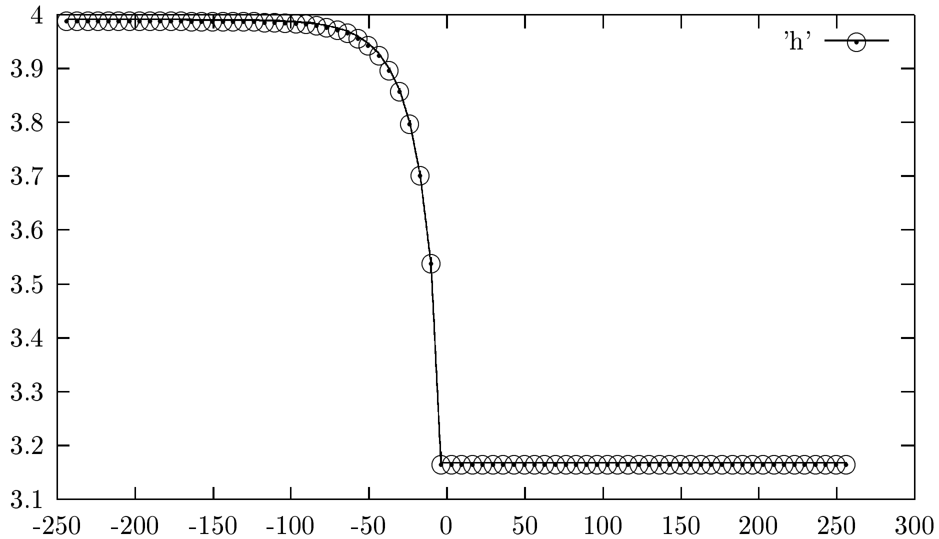
'h'
4
3.9
3.8
3.7
3.6
3.5
3.4
3.3
3.2
3.1
-250
-200
-150
-100
-50
0
50
100
150
200
250
300

## 5.3 Test 2

Here the bed slope values 0.4( hence $\beta_{amont} \simeq \sqrt{2} \simeq 1.414$ ) upstream and 0.01 downstream( hence $\beta_{aval} \simeq \sqrt{0.05} \simeq 0.22$ ). The slope is steep upstream and mild downstream. The flow rate is $101,937 ms^{-1}$. The results are shown after 2495 iterations i.e. $t = 650s$. The steady states downstream and upstream are the ones whished.

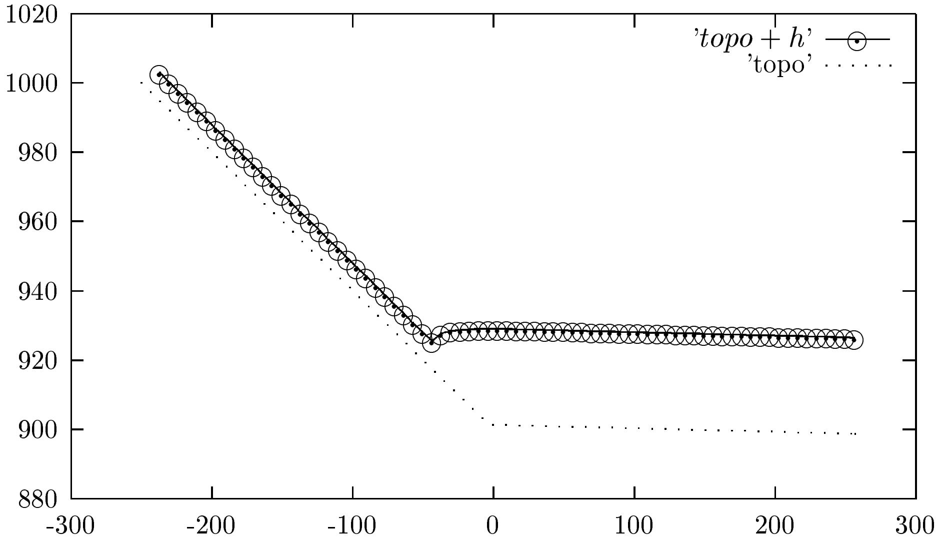


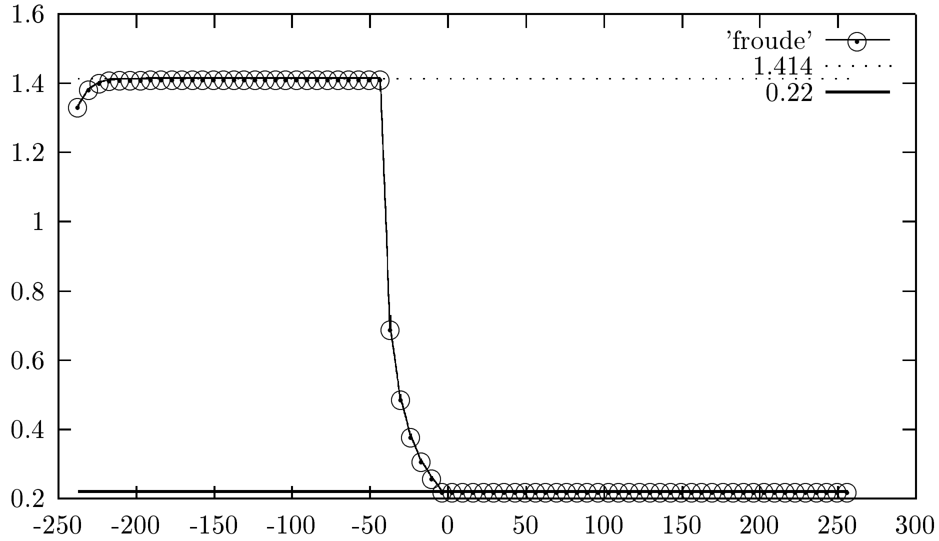


## 5.4 Test 3

Here the bed slope values 0.4( hence $\beta_{amont} \simeq \sqrt{2} \simeq 1.414$ ) upstream and 0.01 downstream( hence $\beta_{aval} \simeq \sqrt{0.05} \simeq 0.22$ ). The bed slope upstream is steep and the bed slope downstream is mild.
The obstacle is of parabolic form and its height is 62.5 metres.
The flow rate is $101,937 ms^{-1}$. The results are shown after 3453 iterations i.e. $t = 1500s$. The steady states upstream and downstream are the ones wished.

An hydraulic jump happens at the downstream of the obstacle. The flow which was supercritical becomes subcritical. One observes the stationary shock at the downward part of the obstacle. The flow is sonic at the top of the obstacle.

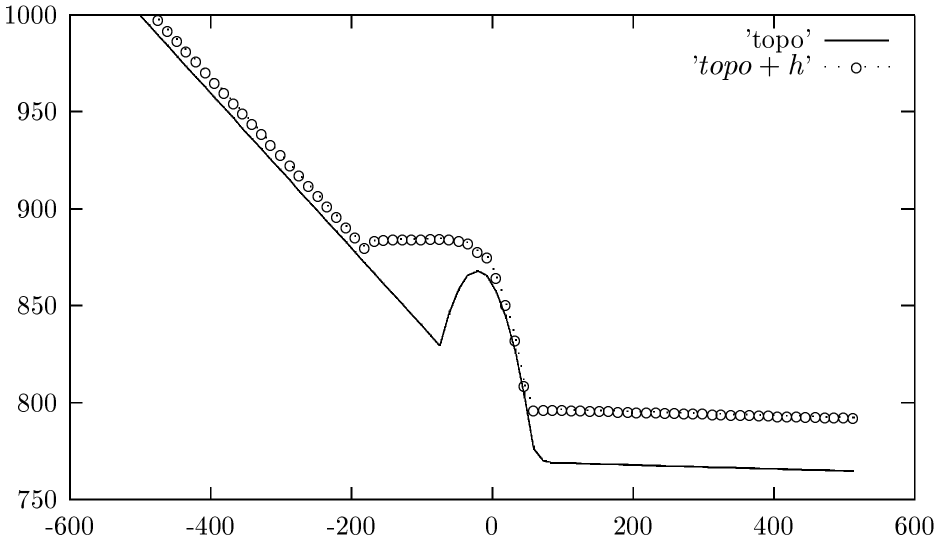


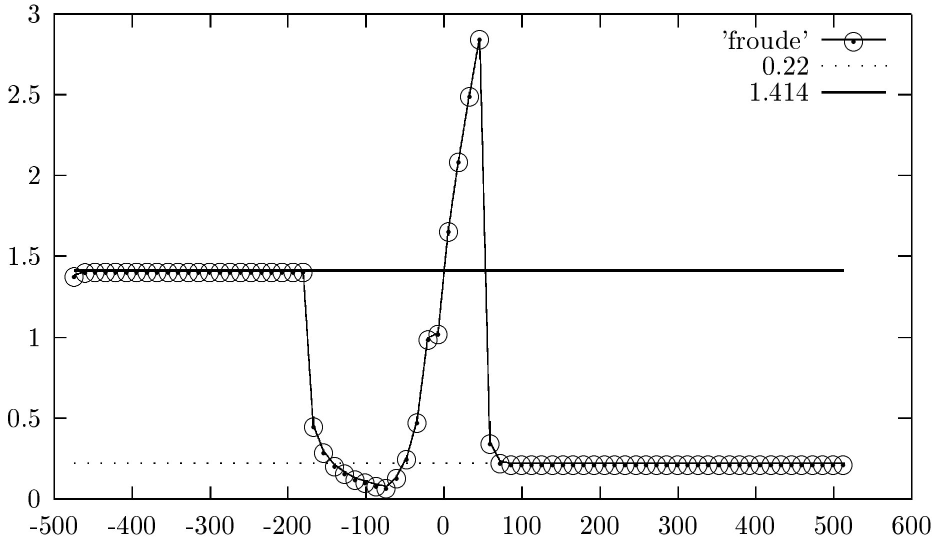


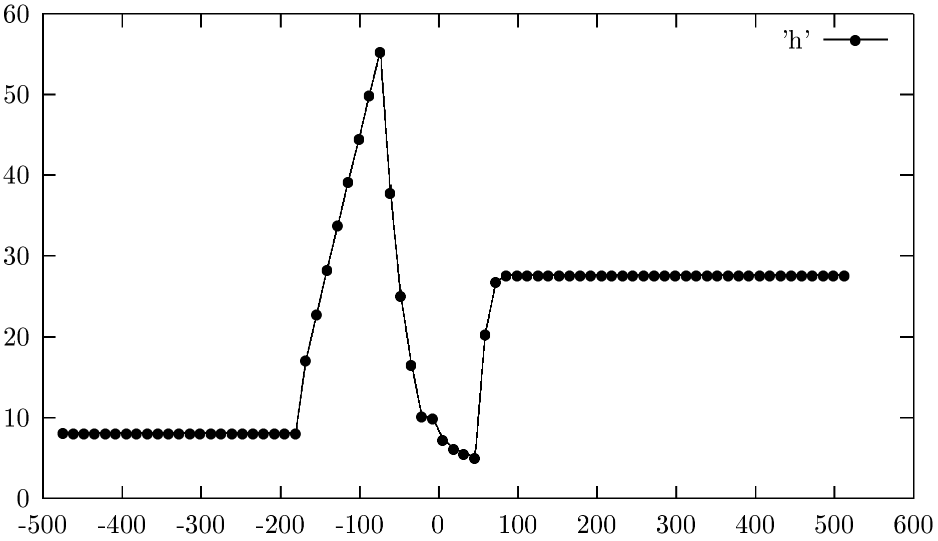

## 5.5 Test 4

Here the bed slope values 0.4( hence $\beta_{amont} \simeq \sqrt{2} \simeq 1.414$ ) upstream and 0.01 downstream( hence $\beta_{aval} \simeq \sqrt{0.05} \simeq 0.22$ ). The slope is steep upstream and mild downstream.
There are two holes. The first one has a depth of 62.5 metres and the second one has a depth of 8.5 metres.
The flow rate is $101,937ms^{-1}$. The results are shown after 4892 iterations of time i.e. $t = 2000s$. The steady states upstream and downstream are the ones wished.

We see in this numerical experience that the downstream flow controls the upstream flow. Indeed $h + a$ remains quasi-constant at the place of the second hole which is not very big. At the place of the first hole, there are stationary shocks.

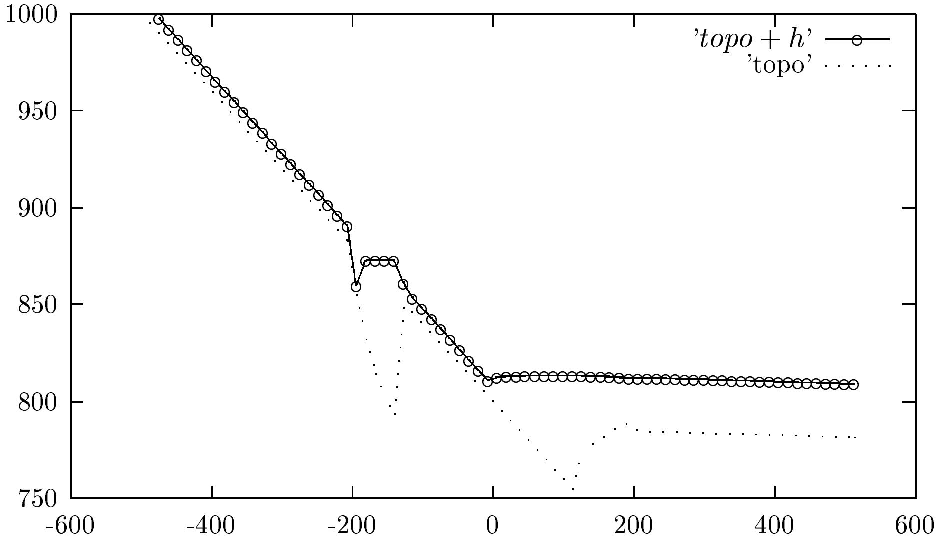


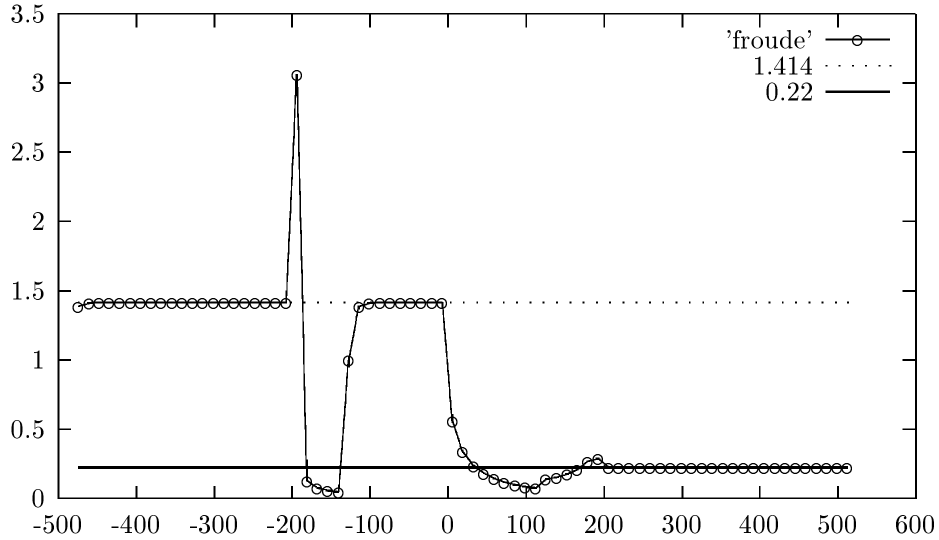

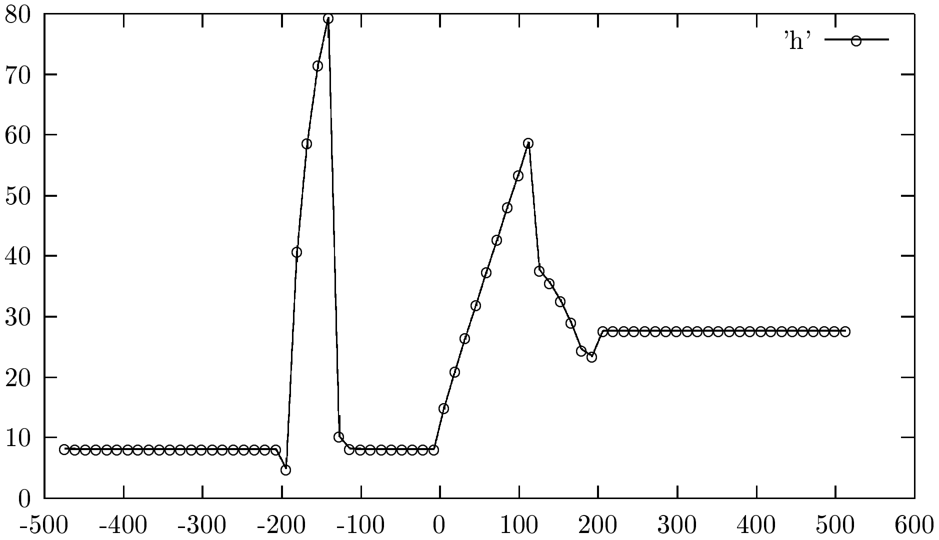


## 5.6 Test 5

We want to see whether the solver can cope with the generation of dry zones. The first figure is shown after one iteration of time, the second after $t = 50s$, the third after $300s$. We can notice what the well balanced solver will not destroy natural equilibrum.

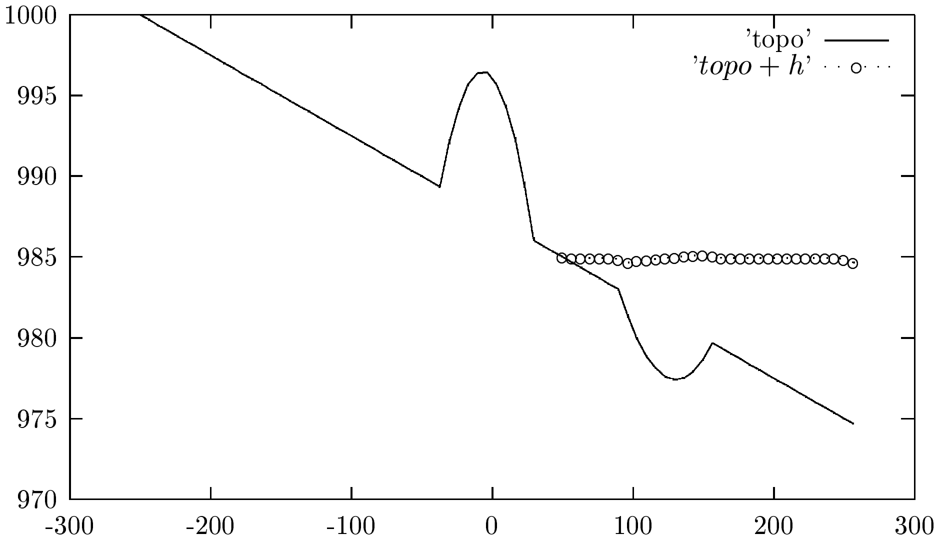

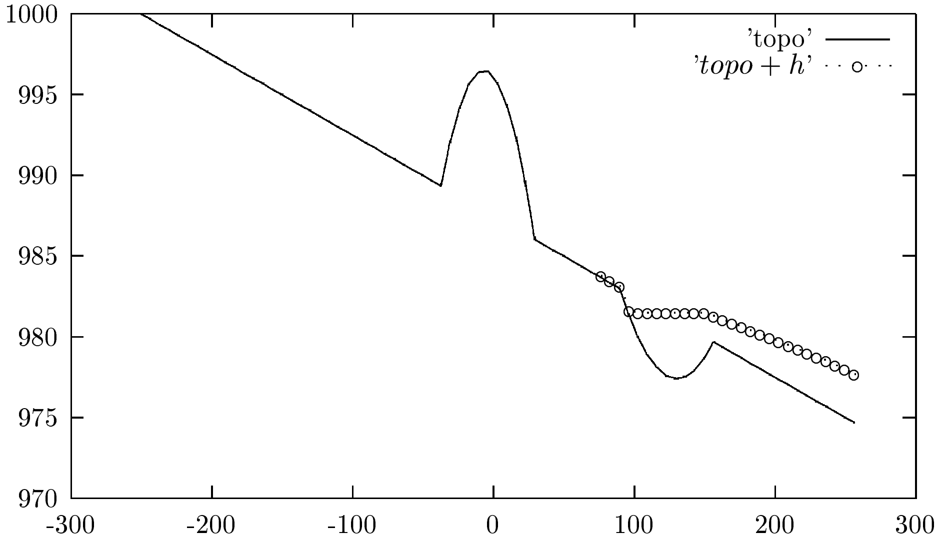


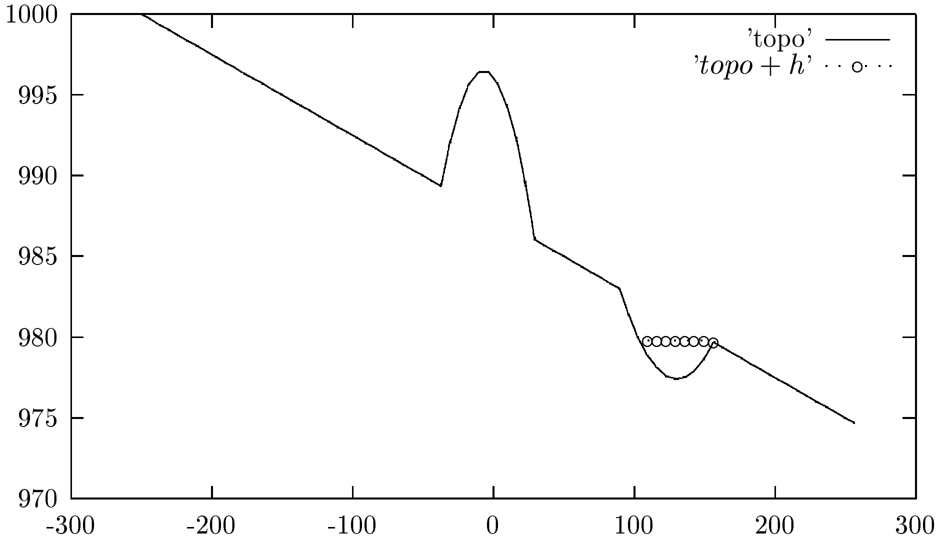


## 5.7 Test 6

We want to see if the solver can cope with flooding dry zones. The figures are shown after $15s$, $400s$, $500s$, $750s$, $1000s$, $1250s$, $2500s$. Upstream are Dirichlet like boundary conditions.

$$h_o = 0.9174 \ ; \ u_o = 0$$

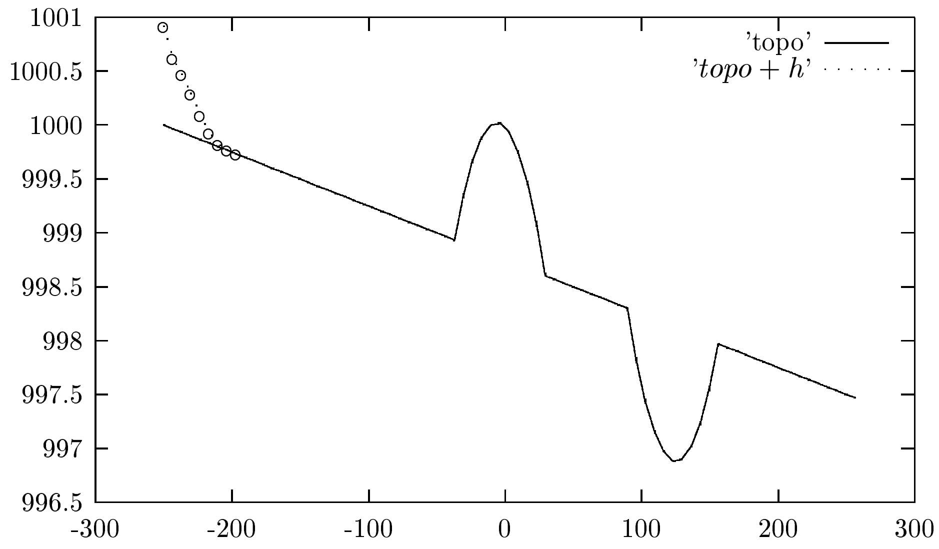
'topo'
'$topo + h$'
1001
1000.5
1000
999.5
999
998.5
998
997.5
997
996.5
-300
-200
-100
0
100
200
300

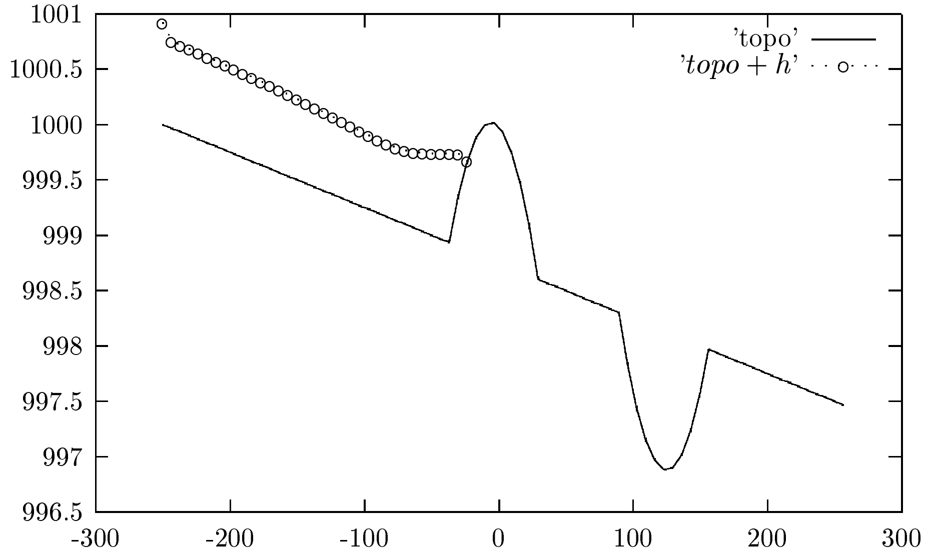
'topo'
'$topo + h$'
1001
1000.5
1000
999.5
999
998.5
998
997.5
997
996.5
-300
-200
-100
0
100
200
300

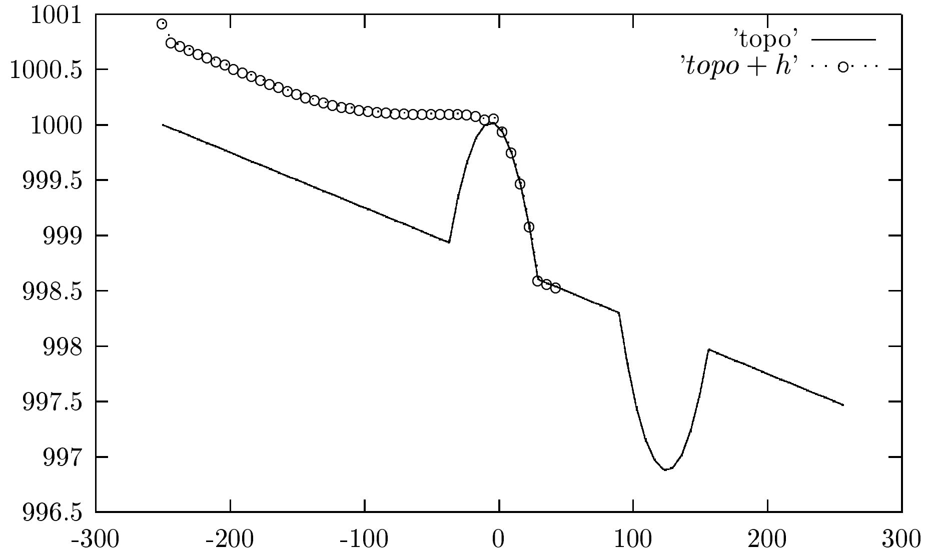
'topo'
'$topo + h$'
1001
1000.5
1000
999.5
999
998.5
998
997.5
997
996.5
-300
-200
-100
0
100
200
300

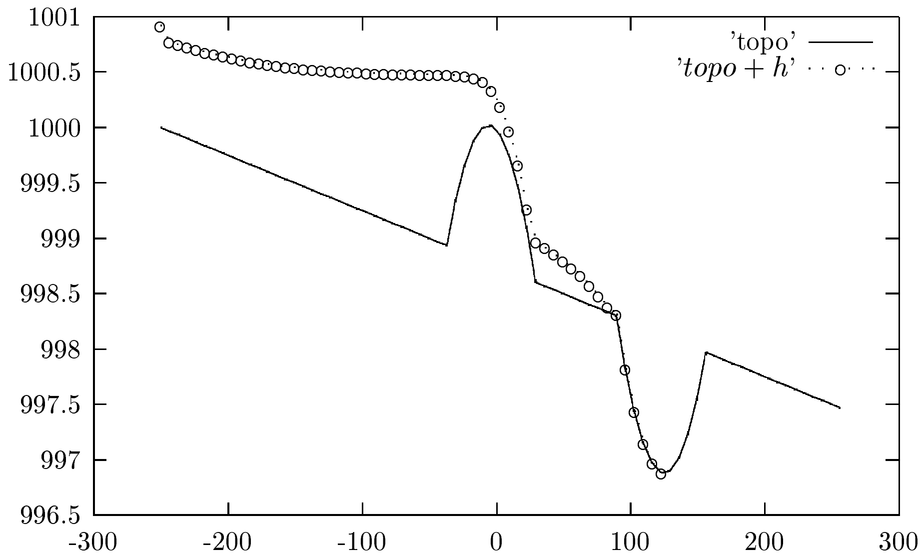
'topo'
'$topo + h$'
1001
1000.5
1000
999.5
999
998.5
998
997.5
997
996.5
-300
-200
-100
0
100
200
300

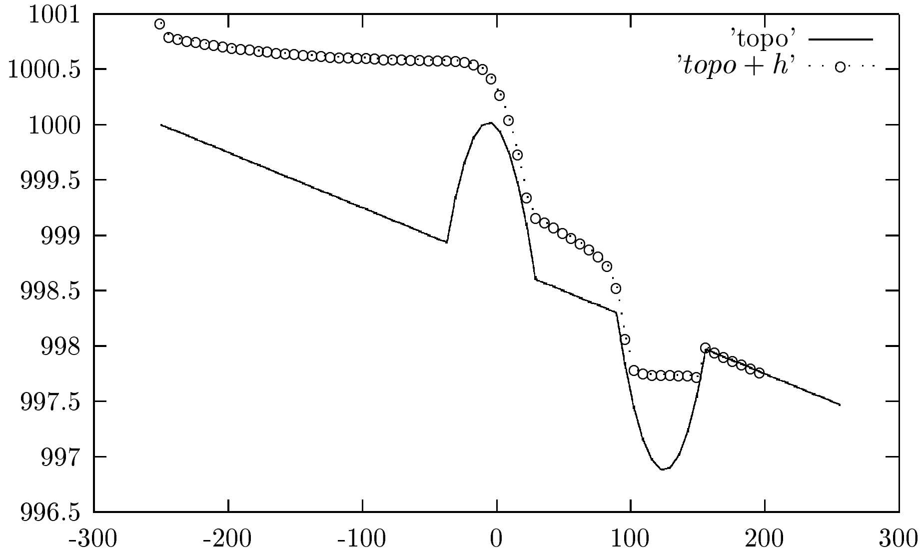
'topo'
'$topo + h$'
1001
1000.5
1000
999.5
999
998.5
998
997.5
997
996.5
-300
-200
-100
0
100
200
300

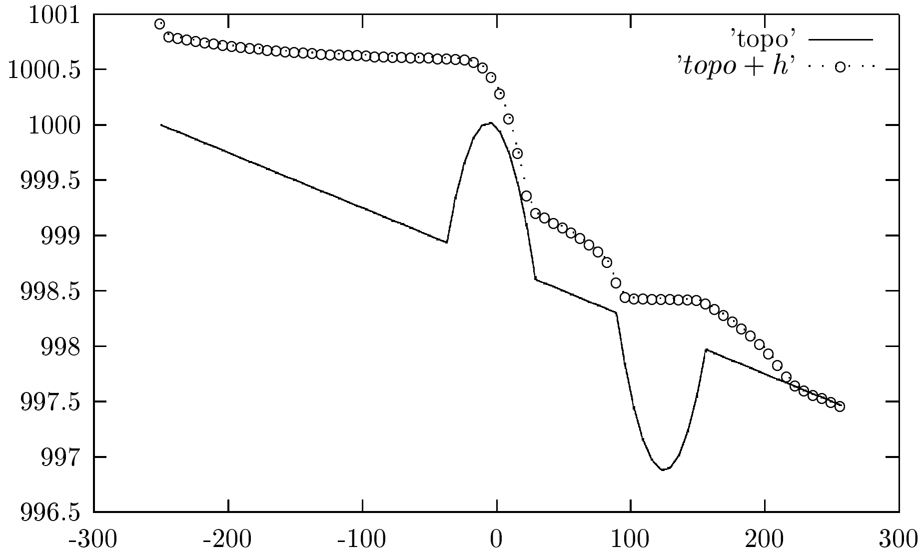
'topo'
'$topo + h$'
1001
1000.5
1000
999.5
999
998.5
998
997.5
997
996.5
-300
-200
-100
0
100
200
300

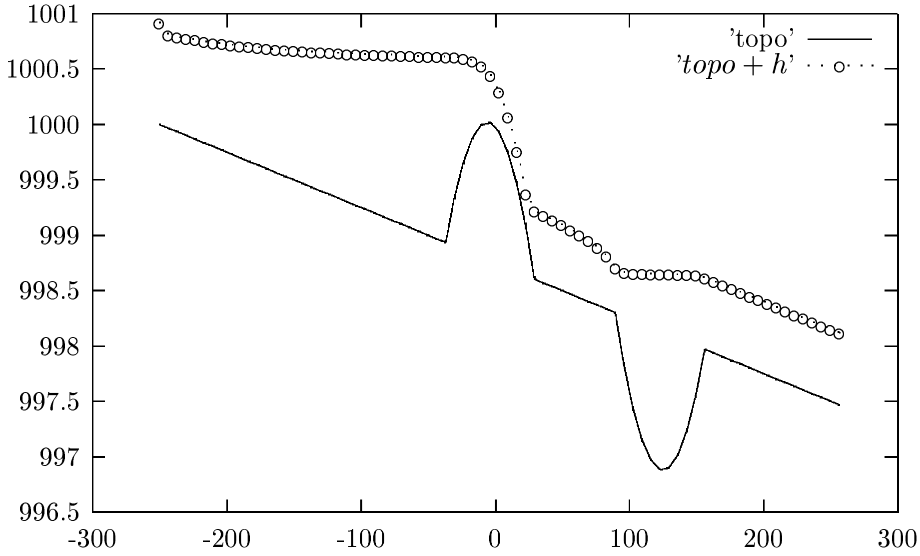

'topo'
'$topo + h$'
1001
1000.5
1000
999.5
999
998.5
998
997.5
997
996.5
-300
-200
-100
0
100
200
300

# Chapter 6

# Some Prospects about the bidimensional model

## 6.1 Physical Model

The two dimensions Shallow Water model can be written as follows

$$
\begin{aligned}
h_t + (hu)_x + (hv)_y &= 0 && (6.1)\\
(hu)_t + (hu^2)_x + (huv)_y + g\Big(\frac{h^2}{2}\Big)_x &= -gha_x - \frac{g}{C^2}u\sqrt{u^2+v^2} && (6.2)\\
(hv)_t + (huv)_x + (hv^2)_y + g\Big(\frac{h^2}{2}\Big)_y &= -gha_y - \frac{g}{C^2}v\sqrt{u^2+v^2} && (6.3)
\end{aligned}
$$

We will pursue the same goal as before. We try to get the relations across the standing wave.
Thereafter, the following model will be considered

$$
\begin{aligned}
h_t + (hu)_x &= 0 && (6.4)\\
(hu)_t + (hu^2)_x + g\Big(\frac{h^2}{2}\Big)_x &= -gha_x - ku\sqrt{u^2+v^2} && (6.5)\\
(hv)_t + (huv)_x &= -kv\sqrt{u^2+v^2} && (6.6)
\end{aligned}
$$

such as $k = \dfrac{g}{C^2}$.

## 6.2 Regular Solutions Analysis

### 6.2.1 Conservative form

The system of equations can be written in a non conservative form as follows

$$
\begin{aligned}
h_t + (hu)_x &= 0 && (6.7)\\
h(u_t + uu_x + gh_x) &= 0 && (6.8)\\
h(v_t + uv_x) &= 0 && (6.9)
\end{aligned}
$$

This hyperbolic system has three eigenvalues : $u-c, u, u+c$ such as $c = \sqrt{gh}$ the sound speed of this hyperbolic system.

### 6.2.2 The Well Balanced Solver

We will again use the formalism of the well balanced solver which has been exposed in the third chapter.

One defines $\theta$

$$u = \sqrt{u^2+v^2}\cos\ \theta$$
$$v = \sqrt{u^2+v^2}\sin\ \theta$$

One writes $u$ as a function of $h$ and one supposes $h \neq 0$. One will place oneself in the configuration of the chapter 3. We consider the coupling between the continuity equation and the dynamic equation in the x-coordinate of the velocity. Thus we get

$$\begin{pmatrix} 1 & (hu)' \\ (hu)' & u^2+2huu'+gh \end{pmatrix}\begin{pmatrix} h_t \\ h_x \end{pmatrix} = \frac{(-1)}{\epsilon}\begin{pmatrix} 0 \\ g\triangle a + k\triangle x u\sqrt{u^2+v^2} \end{pmatrix} \quad (6.10)$$

hence as we are looking for a stationary wave, we obtain

$$\begin{cases} \dfrac{d}{dh}(hu(h)) = 0 \\ \psi'(h)h_x = \dfrac{1}{\epsilon} \end{cases} \quad (6.11)$$

and

$$\psi'(h) = \frac{h_c^3 - h^3}{sk\triangle x\gamma h_c^3 - |\triangle a|h^3} \quad (6.12)$$

such as

$$\begin{cases} h_c^3 = \dfrac{B^2}{g}, B = hu \in \mathbb{R} \text{ the flow rate} \\ s = sgn(B) \\ \gamma = \sqrt{1+\frac{v^2}{u^2}} = \dfrac{1}{|cos\ \theta|} \end{cases} \quad (6.13)$$

We need another equation in order to get the behaviour of $\gamma$. Indeed we need to known one relation for the y-coordinate of the velocity. We consider the coupling between the second dynamic equation and the continuity equation.

$$\begin{pmatrix} 1 & (hu)' \\ (hv)' & (huv)' \end{pmatrix}\cdot\begin{pmatrix} h_t \\ h_x \end{pmatrix} = \begin{pmatrix} 0 \\ -\dfrac{k\triangle x v\sqrt{u^2+v^2}}{\epsilon} \end{pmatrix} \quad (6.14)$$

hence after some manipulations

$$s\frac{hv'}{\gamma v}h_x = -\frac{k\triangle x}{\epsilon} \quad (6.15)$$

As $\epsilon h_x = \dfrac{1}{\psi'(h)}$, we get

$$s\frac{hv'}{\gamma v} = -k\triangle x\frac{h_c^3 - h^3}{sk\triangle x\gamma h_c^3 - |\triangle a|h^3} \quad (6.16)$$

And as $\dfrac{v'}{v} = \dfrac{\gamma\gamma'}{\gamma^2-1} - \dfrac{1}{h}$, after some manipulations we obtain

$$\gamma^2\gamma'(\gamma h_c^3 - s\beta^2 h^3) = (\gamma^2-1)(\gamma - s\beta^2)h^2 \tag{6.17}$$

such as $\beta = \sqrt{\dfrac{|\triangle a|}{k\triangle x}}$. We have obtained a first order ordinary differential equation.

Therefore, when regular solutions are investigated, we integrate the (6.11) and we get the following relations across the standing wave

$$\boxed{\begin{array}{rcl} h_l u_l &=& h_r u_r \\ \psi(h_r) - \psi(h_l) &=& 1 \end{array}}$$

such as

$$\begin{array}{rcl} \psi'(h) &=& \dfrac{h_c^3 - h^3}{sk\triangle x\gamma h_c^3 - |\triangle a|h^3} \\ \gamma^2\gamma'(\gamma h_c^3 - s\beta^2 h^3) &=& (\gamma^2-1)(\gamma - s\beta^2)h^2 \end{array}$$

The $\gamma$-equation is a first order ordinary differential equation which we have not been able to solve analytically. Anyway, we can get its profile. Then we show the $\gamma$ function in all circumstances. As usual $\beta^2 h_o^3 = h_c^3$.

We define $\delta = \dfrac{1}{\gamma} = |cos\ \theta|$

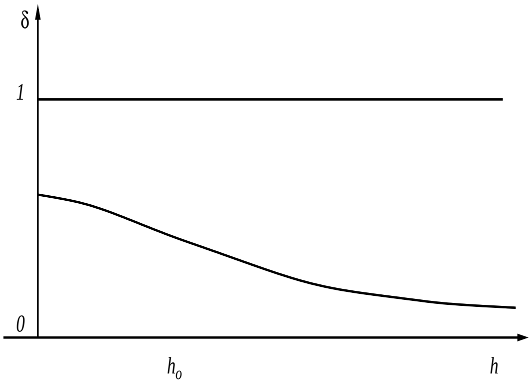


Figure 6.1: $s = -1$

The initial condition for the ordinary differential equation is to be defined. We use the characterics.

When $s = +1$, then the flow rate is positive, hence the wave which velocity is $u$ is positive so $v_l = v_g$.

When $s = -1$, then the flow rate is negative, hence the wave which velocity is $u$ is negative so $v_r = v_d$.

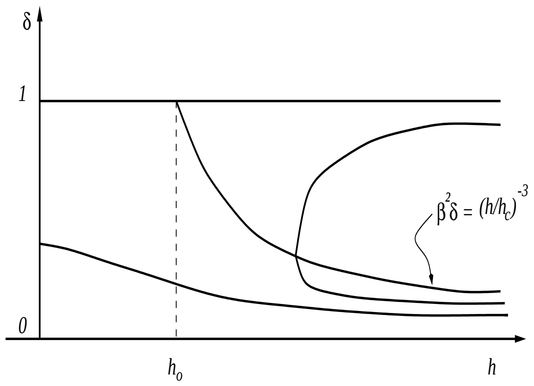


Figure 6.2: $s = 1$ and $\beta < 1$

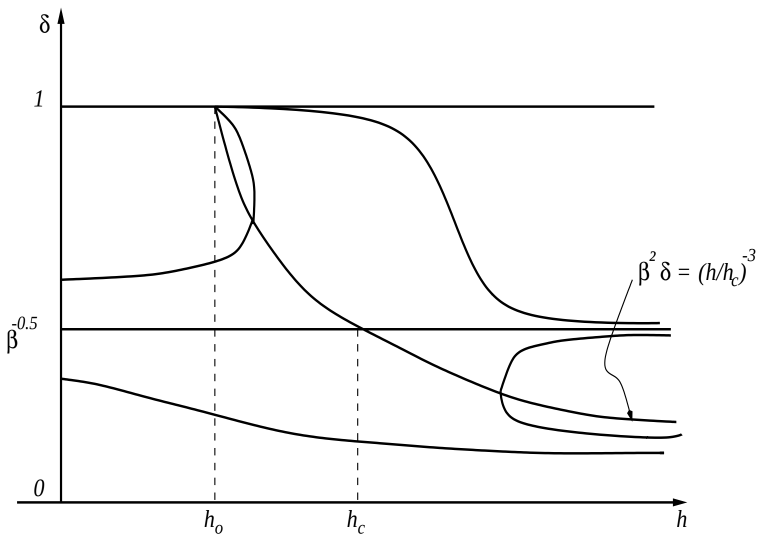


Figure 6.3: $s = 1$ and $\beta > 1$

We remark that

- if $\underline{\beta < 1}$ then the slope is *mild*
- if $\underline{\beta > 1}$ then
  - if $\underline{\gamma > \beta^2}$ then the slope is *mild*
  - if $\underline{\gamma < \beta^2}$ then the slope is *steep*

In the one dimension Shallow Water model, $\delta = 1$ and therefore the curves $u = \beta\sqrt{\delta}c$ were straight lines. In the two dimension model, this is no longer the case. Anyway, the phase plane is declined in the same way.

The numerical method based on a dichotomy can still be used. Anyway one has to known the value of $\gamma$ for the numerical evaluation of $\triangle\psi$. Thus a simple numerical procedure in order to numerically evaluate $\gamma$ is proposed.

If $s = -1$, we choose $L$ and $R$ in the phase plane on the same flow rate. We consider $\gamma_r^2 = 1 + \dfrac{v_d^2}{u_r^2}$ and we numerically integrate $\gamma$ with a backward Euler method in order to get $\gamma_l$. Then we consider $|\triangle\psi - 1|$. One reiterates until convergence. Afterwards $v_r$ can be numerically evaluated.

If $s = +1$, $\beta < 1$ then the slope is mild. And if we are looking for a solution in the phase plane such as $(h_r, h_l) < h_o$, one can choose $\gamma \approx \tilde{\gamma} \approx \gamma_l$ real. Indeed there seems to be no numerical use to integrate $\gamma$. Note that if $\beta^2\delta_l \gtrsim \left(\dfrac{h_c}{h}\right)^3$ then $\triangle\psi \to +\infty$ so $\triangle h \simeq 0$ and one deduces the value of $\delta_r$. If we are looking for a solution in the phase plane such as $(h_r, h_l) > h_o$ and that $\delta_l$ is found to be such as $\beta^2\delta_l \gg \left(\dfrac{h_c}{h}\right)^3$ then $\delta_l \approx \delta_r \approx 1$. Otherwise one takes $\gamma \approx \beta^2\left(\dfrac{h}{h_c}\right)^3$.

Let $s = +1$, $\beta > 1$. Let the slope be mild( $\gamma > \beta^2$ ). Therefore one can use the numerical procedure which has been proposed in the latter paragraph.
Let the slope be steep( $\gamma < \beta^2$ ). On the one hand, if we are looking for a solution in the phase plane such as $(h_r, h_l) < h_o$, one can choose $\gamma \approx \tilde{\gamma} \approx \gamma_l$ real. On the other hand, note that if $\beta^2\delta_l \gtrsim \left(\dfrac{h_c}{h}\right)^3$ then $\triangle\psi \to +\infty$ so $\triangle h \simeq 0$ and one deduces the value of $\delta_r$. If $\beta^2\delta_l \gg \left(\dfrac{h_c}{h}\right)^3$ then one can numerically integrate $\gamma$ with the initial condition $\gamma_l$. Otherwise if $\beta^2\delta_l \approx \left(\dfrac{h_c}{h}\right)^3$, one takes $\gamma \approx \beta^2\left(\dfrac{h_c}{h}\right)^3$. And finally if the latter conditons do not take place, one can numerically integrate $\gamma$.

# Conclusion

A scheme which can handle a great variety of flows has been elaborated. Indeed a finite volume type scheme, with the effects of the source terms of the bottom slope and the friction slope concentrated on the border of each cell has enabled us to deal correctly with the physical model.

Therefore we have been able to simulate smooth transitions as well as hydraulic jumps, we have able to deal with the presence of dry zones as well as its generation. Hence some singularities of an hydraulic flow have been simulated.

In a near future, the conveyance could be introduced in the model and the friction model of Manning-Strickler could be considered whithout any difficulty.
And of course, the bidimensional Shallow Water model is currently under study.

Moreover, these techniques will be introduced in the Rozabel code [7].

# Bibliography


[1] C. Bon. *Modélisation et simulation numérique d'écoulements hydrauliques et de ruisselement en topographie quelconque.* PhD thesis, University Bordeaux I, 1997.

[2] V.T. Chow. *Open-Channel hydraulics*, New-York, McGraw-Hill, 1959.

[3] J.M. Greenberg and A.Y. Le Roux. *A well balanced scheme for the processing of source terms in hyperbolic equations.* SIAM, Journal of Numerical Analysis, 33(1):1-16, 1996.

[4] O. Lecoz. *Un schéma équilibre pour les écoulements à surface libre instationnaires avec bathymétrie.* PhD thesis, University Bordeaux I, 1996.

[5] A. Lencastre *Manuel d'hydraulique Générale*, Collection de la direction des études et recherches d'électricité de France.

[6] A.Y. Le Roux. *Discrétisation des termes source raides dans les problèmes hyperboliques*, publication INRIA ( mars 1998 ).

[7] N. Seguin. *Génération et Validation de ROZAVEL, un code hydraulique 2D*, rapport de DEA, juin 1999.

[8] J.J. Stocker. *Water Waves*, Interscience Publishers N.Y. 1957.